Table II. Synthetic oligopeptides used in this study

Peptide	Sequence
Tax103–127	P S F L Q A M R K Y S P F R N G Y M E P T L G Q H
Tax120–144	M E P T L G Q H L P T L S F P D P G L R P Q N L Y
Tax137–161	G L R P Q N L Y T L W G G S V V C M Y L Y Q L S P
Tax154–178	M Y L Y Q L S P P I T W P L L P H V I F C H P G Q
Tax171–195	V I F C H P G Q L G A F L T N V P Y K R I E E L L
Tax188–212	Y K R I E E L L Y K I S L T T G A L I I L P E D C
Tax205–229	L I I L P E D C L P T T L F Q P A R A P V T L T A
Tax222–246	R A P V T L T A W Q N G L L P F H S T L T T P G I
Tax146–160	L W G G S V V C M Y L Y Q L S
Tax151–165	V V C M Y L Y Q L S P P I T W
Tax154–168	M Y L Y Q L S P P I T W P L L
Tax155–169	Y L Y Q L S P P I T W P L L P
Tax156–170	L Y Q L S P P I T W P L L P H
Tax161–175	P P I T W P L L P H V I F C H
Tax166–180	P L L P H V I F C H P G Q L G
Tax155–168	Y L Y Q L S P P I T W P L L
Tax155–167	Y L Y Q L S P P I T W P L
Tax155–166	Y L Y Q L S P P I T W P

Tax155–167-specific CD4$^+$ T cells were detected ex vivo in the patient #350 (0.11%) and proliferated to 11.6% among CD4$^+$ T cells at 13 d poststimulation with Tax155–167 peptide. In the patient #364, tetramer-binding CD4$^+$ T cells were undetectable in fresh PBMCs but expanded to 0.37% by in vitro stimulation with Tax155–167 peptide (Fig. 6A). In an HLA-DRB1*0101$^+$–seronegative donor #365, Tax155–167-specific CD4$^+$ T cells were not found in fresh PBMCs and did not become detectable at 13 d after stimulation with Tax155–167 peptide (Fig. 6A). This result indicates that Tax155–167-specific CD4$^+$ T cells are maintained and possesses the abilities to proliferate in response to HTLV-1 Tax in these patients.

We further examined whether Tax155–167-specific CD4$^+$ T cells existed in two HTLV-1–infected individuals carrying HLA-DRB1*0101, an AC #310 and a HAM/TSP patient #294, and detected 0.18 and 0.31% of tetramer-binding cells in peripheral CD4$^+$ T cells, respectively (Fig. 6B). These results suggest that Tax155–167-specific CD4$^+$ T cells are maintained in HTLV-1–infected individuals expressing an HLA-DRB1*0101 allele, regardless of HSCT.

Discussion

In this study, we demonstrated Tax-specific CD4$^+$ T cell responses in some ATL patients post–allo-HSCT and identified a novel HLA-DRB1*0101–restricted CD4 T cell epitope, Tax155–167, which was recognized by HTLV-1–specific CD4$^+$ T cells and consequently led to robust Tax-specific CD8$^+$ T cell expansion. We also found that Tax155–167-specific CD4$^+$ T cells existed in all HTLV-1–infected HLA-DRB1*0101$^+$ individuals tested, regardless of HSCT, by newly generated HLA-DRB1*0101/Tax155–167 tetramers. These results suggest that Tax155–167 might be a dominant epitope recognized by HTLV-1–specific CD4$^+$ T cells

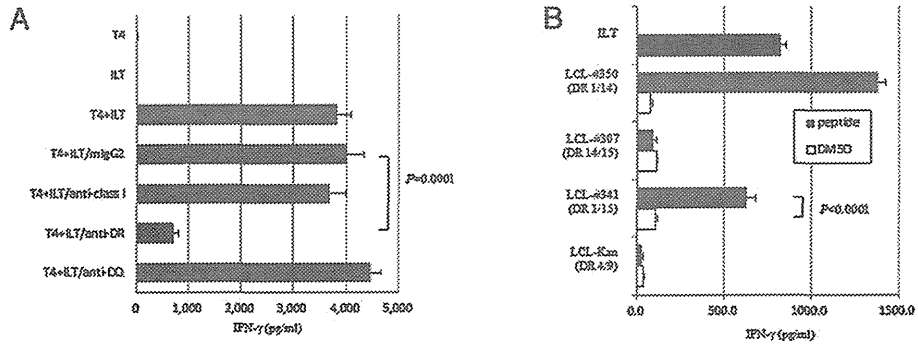

C

	Relative position												
	1	2	3	4	5	6	7	8	9	10	11	12	13
Tax155-167	Y	L	Y	Q	L	S	P	P	I	T	W	P	L
Anchor residues	Y,V, L,F, I,A M,W	*	*	L,A, I,V, M,N, Q	*	A,G, S,T, P	*	*	L,A, I,V, N,F, Y				

FIGURE 4. HLA-DRB1*0101 restriction of Tax155–167 recognition by established T4 cells. (**A**) T4 cells were cocultured for 6 h with ILT-#350 in the presence or absence of the following blocking Abs (10 μg/ml): anti-human HLA-DR; anti-human HLA-DQ; anti–HLA-class I; or isotype control. IFN-γ production from T4 cells was measured by ELISA. (**B**) The T4 cells were cocultured for 6 h with autologous (#350) or allogeneic (#307, #341, and Kan) LCLs pulsed with (closed bar) or without (open bar) Tax155–167 for 1 h or with recipient-derived ILT-#350. The HLA-DR alleles of each LCL line are indicated in parentheses. IFN-γ production of T4 cells was assessed by ELISA. (A and B) Representative data of three independent experiments are shown. The error bars represent SD of triplicate wells. Statistical significance was analyzed by the unpaired *t* test. (**C**) The amino acid sequence between residues 155 and 167 of Tax contained a putative HLA-DRB1*0101 anchor motif (33).

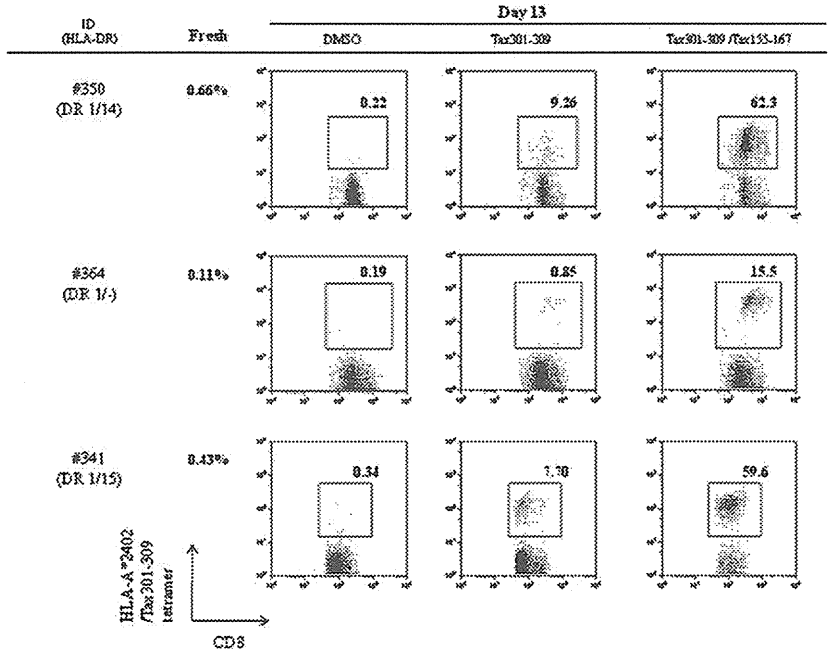

FIGURE 5. Augmentation of Tax-specific $CD8^+$ T cell expansion by costimulation with CTL epitope and Tax155–167 peptides. PBMCs from HLA-DRB1*0101– and HLA-A24–expressing ATL patients (#350, #364, and #341) who underwent allo-HSCT with RIC were cultured for 13 d in the presence of DMSO, 100 nM CTL epitope (Tax301–309), or a mixture of Tax301–309 (100 nM) and Tax155–167 (100 nM) peptides. Data indicate percentages of HLA-A*2402/Tax301–309 $tetramer^+$ cells among $CD3^+CD8^+$ T cells. Fresh indicates frequency of HLA-A*2402/Tax301–309 $tetramer^+CD8^+$ T cells detected in fresh peripheral blood.

in HTLV-1–infected individuals expressing HLA-DRB1*0101 and that Tax-specific $CD4^+$ T cells might efficiently induce HTLV-1–specific CTL expansion to strengthen the graft-versus-ATL effects in ATL patients after allo-HSCT.

In HTLV-1 infection, analysis of virus-specific $CD4^+$ T cell responses appears to be limited because $CD4^+$ T cells are preferentially infected with HTLV-1 (24, 34, 35), and HTLV-1 Ags are produced from infected cells at a few hours postculture (34, 36). In this study, we used blood samples from 18 ATL patients after allo-HSCT with RIC and from HLA identical–related or unrelated donors and found that these recipients had undetectable or very low proviral loads (Table I), as previously shown (7–9). We previously reported that Tax-specific CTLs were induced in some patients with complete remission after allo-HSCT for ATL and might contribute to the graft-versus-leukemia effect (10). In the current study, Tax-specific T cell responses or tetramer-binding $CD8^+$ T cells were detected in 68.8% (11 of 16) or 82.4% (14 of 17) of patients tested, respectively (Fig. 1A, Table I). In addition, helper function of Tax-specific $CD4^+$ T cells to enhance Tax-specific $CD8^+$ T cell expansion was observed in PBMCs from all three HLA-DRB1*0101^+ patients tested (Fig. 5). These data suggest that both $CD8^+$ and $CD4^+$ Tax-specific T cell responses might contribute to elimination of remaining leukemic and/or infected cells in some patients having T cell responses against Tax. However, given the fact that not all ATL patients who achieved complete remission after allo-HSCT had Tax-specific $CD8^+$ T cells, graft-versus-host reaction may mainly contribute to achieve complete remission after allo-HSCT. It is of note that Tax-specific

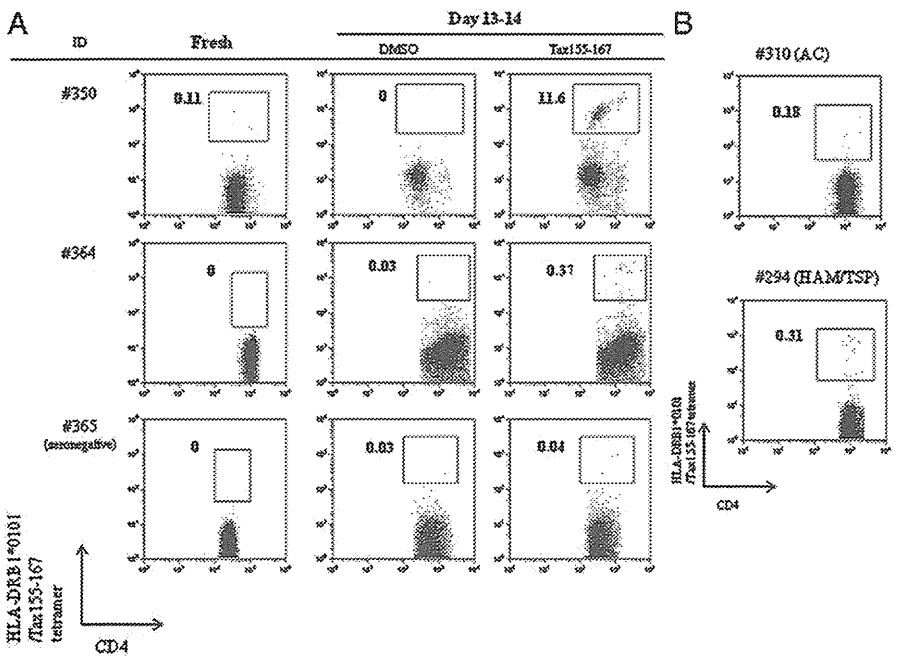

FIGURE 6. Detection of Tax155–167-specific $CD4^+$ T cells in HTLV-1–infected HLA-DRB1*0101^+ individuals. (**A**) In two ATL patients after allo-HSCT (#350 and #364) and an HLA-DRB1*0101^+–seronegative donor (#365), frequency of HLA-DRB1*0101/Tax155–167 tetramer-binding $CD4^+$ T cells was analyzed in fresh PBMCs and PBMCs cultured for 13–14 d in the presence of Tax155–167 (100 nM) peptide. Data indicate percentages of $tetramer^+$ cells in $CD3^+CD4^+$ T cells. (**B**) Frequency of HLA-DRB1*0101/Tax155–167 tetramer-binding $CD4^+$ T cells in fresh PBMCs from an AC #310 and an HAM/TSP patient #294 was analyzed. Data indicate percentages of $tetramer^+$ cells in $CD3^+CD4^+$ T cells.

T cell responses were detected in 57.1% (four of seven) or 87.5% (seven of eight) of the patients after allo-HSCT with RIC from HTLV-1–seronegative sibling or unrelated donors, respectively. A Tax-specific T cell response was not detected in three patients who underwent allo-HSCT from seropositive donors (Fig. 1, Table I).

It has been proposed that CTLs are the main effector cells against many pathogenic viruses, including HTLV-1. To date, many CTL epitopes recognized by HTLV-1–specific CTLs have been identified, some of which are thought to be the candidates of peptide-based T cell immunotherapy (10, 20, 32, 37–40). $CD4^+$ T cells have also been known to be critical for induction and maintenance of Ag-specific $CD8^+$ T cells (15–19). With respect to HTLV-1 infection, there are several reports identifying HLA-DRB1*0101–restricted epitopes recognized by $CD4^+$ T cells against Env or Tax (Env380–394 (21), Env436–450, Env451–465, Env456–470 (23), and Tax191–205 (22)), which were established by stimulating PBMCs from uninfected or infected individuals with synthetic peptides. In this study, for determination of an epitope recognized by HTLV-1–specific $CD4^+$ T cells, we established an HTLV-1–specific $CD4^+$ T cell line from the patient #350 at 180 d after allo-HSCT by several stimulations with an HTLV-1 Ags-expressing T cell line (ILT-#350) from the same patient. In addition, we found that Tax155–167-specific $CD4^+$ T cells were present in peripheral blood from patient #350 at 180 and 540 d after all-HSCT, indicating that the epitope, Tax155–167, identified in this study is naturally presented on HTLV-1–infected cells and predominantly recognized by HTLV-1–specific $CD4^+$ Th cells in the patient #350 at least within 540 d after allo-HSCT. Another HLA-DRB1*0101–restricted Tax epitope, Tax191–205, has been reported previously (22). In this study, the amino acid sequence within this region was revealed to be conserved in the infected T cell line, ILT-#350 established from the patient #350 (data not shown), indicating that Tax191–205 can be presented on APCs and Tax191–205-specific $CD4^+$ T cells may be induced in patient #350. However, Tax155–167-specific but not Tax191–205-specific $CD4^+$ T cells were revealed to predominantly appear in the HTLV-1–specific T4 cell line, established from PBMCs in the patient #350 at 180 d after allo-HSCT. This suggests that in the case of patient #350 at 180 d after allo-HSCT, Tax191–205-specific $CD4^+$ T cells may not be the most frequent population among HTLV-1–specific $CD4^+$ T cells.

It has been known that Ag-specific effector and memory $CD4^+$ T cells are typically present at much lower frequencies than their $CD8^+$ counterparts and that MHC class II tetramer might have a weak TCR–MHC affinity (41). Although this limited affinity of MHC class II tetramer might preclude detection of Ag-specific low-affinity $CD4^+$ T cells, the low-affinity $CD4^+$ T cells, below detection with MHC class II tetramers, were also proved to be critical effectors in Ag-specific responses (42). In the current study, MHC class II tetramer analysis revealed that Tax155–167-specific $CD4^+$ T cells were present in HLA-DRB1*0101^+ HTLV-1–infected individuals: two ATL patients after allo-HSCT (day 180 for #350 and day 360 for #364), an AC #310, and a HAM/TSP patient #294 (Fig. 6). Because of a shortage of blood sample from patient #341, we could not perform the direct detection for Tax155–167-specific $CD4^+$ T cells by the MHC class II tetramers. However, enhanced expansion of Tax301–309-specific $CD8^+$ T cells was observed in patient #341 at 360 d after allo-HSCT when PBMCs were stimulated with Tax301–309 in the presence of Tax155–167 (Fig. 5). So far, Tax155–167-specific $CD4^+$ T cells were detected in fresh and/or Tax155–167-stimulated PBMCs of all HTLV-1–infected HLA-DRB1*0101^+ individuals tested, although their frequencies were various. These results suggest that Tax155–167 may be the dominant epitope recognized by Tax-specific $CD4^+$ T cells in HTLV-1–infected HLA-DRB1*0101^+ individuals. In ATL patients after HSCT, the donor-derived T cells reconstituted in recipients will first encounter HTLV-1 Ags, because HTLV-1 still persists in the patients even though proviral loads become undetectable in the peripheral bloods. Indeed, we found that donor-derived Tax155–167-specific $CD4^+$ T cells were present in three ATL patients after allo-HSCT from seronegative donors. This finding also suggests that Tax155–167-specific naive $CD4^+$ T cells may pre-exist in HLA-DRB1*0101^+ individuals and can be primed with HTLV-1 Ags during the primary infection. In this study, Tax155–167-specific $CD4^+$ T cells were also detected in an AC and a HAM/TSP patient (Fig. 6B), suggesting that Tax155–167-specific $CD4^+$ T cells may be maintained in some HLA-$DR1^+$ individuals during the chronic phase of HTLV-1 infection. However, it has been reported that epitope hierarchies may change because of T cell escape mutants (43, 44) and unresponsiveness or deletion of epitope-specific T cells because of prolonged Ag stimulation during chronic infection (45, 46). Further longitudinal studies with a number of samples will be required to confirm that Tax155–167 is a dominant epitope of HTLV-1–specific $CD4^+$ T cells in HLA-DRB1*0101^+–infected individuals in the course of HTLV-1 infection.

Among three patients (#241, #350, and #364) showing high T cell responses against recombinant Tax protein, two patients (#350 and #364) were found to carry HLA-DRB1*0101 and have efficient $CD4^+$ Th cell responses against Tax155–167. Intriguingly, it has been reported that HLA-DRB1*0101 is associated with susceptibility to HAM/TSP (47, 48). In addition, $CD4^+$ T cells have been shown to be the dominant cells infiltrating in early active inflammatory spinal cord lesions (28, 29) with spontaneous production of proinflammatory cytokines (30). These observations suggest that HLA-DRB1*0101 might be associated with susceptibility to HAM/TSP via an effect on high $CD4^+$ T cell activation. Further studies are needed to clarify whether HLA-DRB1*0101 is associated with high Tax-specific $CD4^+$ T cell responses in HTLV-1–infected individuals.

Early studies using lymphocytic choriomeningitis virus showed that $CD4^+$ T cell help is critical for maintenance of $CD8^+$ T cell function during chronic infections (18). It has also been suggested that $CD4^+$ T cells are required for optimal CTL responses during HTLV-1 infection (49). Aubert et al. (50) showed that both Ag-specific naive and effector $CD4^+$ T cell help rescued exhausted $CD8^+$ T cells in vivo, resulting in a decrease in viral burden. In the current study, we determined a novel HLA-DRB1*0101–restricted Th epitope, Tax155–167, which was capable of augmenting Tax-specific $CD8^+$ T cell expansion by stimulating Tax155–167-specific $CD4^+$ T cells. This epitope would be a useful tool for investigating the roles of HTLV-1–specific $CD4^+$ T cells in antitumor immunity and in pathogenesis of HTLV-1–related inflammatory diseases such as HAM/TSP and developing novel vaccines to prevent progression or recurrence of ATL.

Disclosures

The authors have no financial conflicts of interest.

References

1. Hinuma, Y., K. Nagata, M. Hanaoka, M. Nakai, T. Matsumoto, K. I. Kinoshita, S. Shirakawa, and I. Miyoshi. 1981. Adult T-cell leukemia: antigen in an ATL cell line and detection of antibodies to the antigen in human sera. *Proc. Natl. Acad. Sci. USA* 78: 6476–6480.
2. Poiesz, B. J., F. W. Ruscetti, A. F. Gazdar, P. A. Bunn, J. D. Minna, and R. C. Gallo. 1980. Detection and isolation of type C retrovirus particles from fresh and cultured lymphocytes of a patient with cutaneous T-cell lymphoma. *Proc. Natl. Acad. Sci. USA* 77: 7415–7419.

3. de Thé, G., and R. Bomford. 1993. An HTLV-I vaccine: why, how, for whom? *AIDS Res. Hum. Retroviruses* 9: 381–386.
4. Uchiyama, T. 1997. Human T cell leukemia virus type I (HTLV-I) and human diseases. *Annu. Rev. Immunol.* 15: 15–37.
5. Tsukasaki, K., T. Maeda, K. Arimura, J. Taguchi, T. Fukushima, Y. Miyazaki, Y. Moriuchi, K. Kuriyama, Y. Yamada, and M. Tomonaga. 1999. Poor outcome of autologous stem cell transplantation for adult T cell leukemia/lymphoma: a case report and review of the literature. *Bone Marrow Transplant.* 23: 87–89.
6. Utsunomiya, A., Y. Miyazaki, Y. Takatsuka, S. Hanada, K. Uozumi, S. Yashiki, M. Tara, F. Kawano, Y. Saburi, H. Kikuchi, et al. 2001. Improved outcome of adult T cell leukemia/lymphoma with allogeneic hematopoietic stem cell transplantation. *Bone Marrow Transplant.* 27: 15–20.
7. Tanosaki, R., N. Uike, A. Utsunomiya, Y. Saburi, M. Masuda, M. Tomonaga, T. Eto, M. Hidaka, M. Harada, I. Choi, et al. 2008. Allogeneic hematopoietic stem cell transplantation using reduced-intensity conditioning for adult T cell leukemia/lymphoma: impact of antithymocyte globulin on clinical outcome. *Biol. Blood Marrow Transplant.* 14: 702–708.
8. Choi, I., R. Tanosaki, N. Uike, A. Utsunomiya, M. Tomonaga, M. Harada, T. Yamanaka, M. Kannagi, and J. Okamura. 2011. Long-term outcomes after hematopoietic SCT for adult T-cell leukemia/lymphoma: results of prospective trials. *Bone Marrow Transplant.* 46: 116–118.
9. Okamura, J., A. Utsunomiya, R. Tanosaki, N. Uike, S. Sonoda, M. Kannagi, M. Tomonaga, M. Harada, N. Kimura, M. Masuda, et al. 2005. Allogeneic stem-cell transplantation with reduced conditioning intensity as a novel immunotherapy and antiviral therapy for adult T-cell leukemia/lymphoma. *Blood* 105: 4143–4145.
10. Harashima, N., K. Kurihara, A. Utsunomiya, R. Tanosaki, S. Hanabuchi, M. Masuda, T. Ohashi, F. Fukui, A. Hasegawa, T. Masuda, et al. 2004. Graft-versus-Tax response in adult T-cell leukemia patients after hematopoietic stem cell transplantation. *Cancer Res.* 64: 391–399.
11. Jacobson, S., H. Shida, D. E. McFarlin, A. S. Fauci, and S. Koenig. 1990. Circulating $CD8^+$ cytotoxic T lymphocytes specific for HTLV-I pX in patients with HTLV-I associated neurological disease. *Nature* 348: 245–248.
12. Kannagi, M., S. Harada, I. Maruyama, H. Inoko, H. Igarashi, G. Kuwashima, S. Sato, M. Morita, M. Kidokoro, M. Sugimoto, et al. 1991. Predominant recognition of human T cell leukemia virus type I (HTLV-I) pX gene products by human $CD8^+$ cytotoxic T cells directed against HTLV-I-infected cells. *Int. Immunol.* 3: 761–767.
13. Shimizu, Y., A. Takamori, A. Utsunomiya, M. Kurimura, Y. Yamano, M. Hishizawa, A. Hasegawa, F. Kondo, K. Kurihara, N. Harashima, et al. 2009. Impaired Tax-specific T-cell responses with insufficient control of HTLV-1 in a subgroup of individuals at asymptomatic and smoldering stages. *Cancer Sci.* 100: 481–489.
14. Takamori, A., A. Hasegawa, A. Utsunomiya, Y. Maeda, Y. Yamano, M. Masuda, Y. Shimizu, Y. Tamai, A. Sasada, N. Zeng, et al. 2011. Functional impairment of Tax-specific but not cytomegalovirus-specific $CD8^+$ T lymphocytes in a minor population of asymptomatic human T-cell leukemia virus type 1-carriers. *Retrovirology* 8: 100.
15. Cardin, R. D., J. W. Brooks, S. R. Sarawar, and P. C. Doherty. 1996. Progressive loss of $CD8^+$ T cell-mediated control of a gamma-herpesvirus in the absence of $CD4^+$ T cells. *J. Exp. Med.* 184: 863–871.
16. Grakoui, A., N. H. Shoukry, D. J. Woollard, J. H. Han, H. L. Hanson, J. Ghrayeb, K. K. Murthy, C. M. Rice, and C. M. Walker. 2003. HCV persistence and immune evasion in the absence of memory T cell help. *Science* 302: 659–662.
17. Kalams, S. A., S. P. Buchbinder, E. S. Rosenberg, J. M. Billingsley, D. S. Colbert, N. G. Jones, A. K. Shea, A. K. Trocha, and B. D. Walker. 1999. Association between virus-specific cytotoxic T-lymphocyte and helper responses in human immunodeficiency virus type 1 infection. *J. Virol.* 73: 6715–6720.
18. Matloubian, M., R. J. Concepcion, and R. Ahmed. 1994. $CD4^+$ T cells are required to sustain $CD8^+$ cytotoxic T-cell responses during chronic viral infection. *J. Virol.* 68: 8056–8063.
19. Smyk-Pearson, S., I. A. Tester, J. Klarquist, B. E. Palmer, J. M. Pawlotsky, L. Golden-Mason, and H. R. Rosen. 2008. Spontaneous recovery in acute human hepatitis C virus infection: functional T-cell thresholds and relative importance of CD4 help. *J. Virol.* 82: 1827–1837.
20. Jacobson, S., J. S. Reuben, R. D. Streilein, and T. J. Palker. 1991. Induction of $CD4^+$, human T lymphotropic virus type-1-specific cytotoxic T lymphocytes from patients with HAM/TSP: recognition of an immunogenic region of the gp46 envelope glycoprotein of human T lymphotropic virus type-1. *J. Immunol.* 146: 1155–1162.
21. Kitze, B., K. Usuku, Y. Yamano, S. Yashiki, M. Nakamura, T. Fujiyoshi, S. Izumo, M. Osame, and S. Sonoda. 1998. Human $CD4^+$ T lymphocytes recognize a highly conserved epitope of human T lymphotropic virus type 1 (HTLV-1) env gp21 restricted by HLA DRB1*0101. *Clin. Exp. Immunol.* 111: 278–285.
22. Kobayashi, H., T. Ngato, K. Sato, N. Aoki, S. Kimura, Y. Tanaka, H. Aizawa, M. Tateno, and E. Celis. 2006. In vitro peptide immunization of target tax protein human T-cell leukemia virus type 1-specific $CD4^+$ helper T lymphocytes. *Clin. Cancer Res.* 12: 3814–3822.
23. Yamano, Y., B. Kitze, S. Yashiki, K. Usuku, T. Fujiyoshi, T. Kaminagayoshi, K. Unoki, S. Izumo, M. Osame, and S. Sonoda. 1997. Preferential recognition of synthetic peptides from HTLV-I gp21 envelope protein by HLA-DRB1 alleles associated with HAM/TSP (HTLV-I-associated myelopathy/tropical spastic paraparesis). *J. Neuroimmunol.* 76: 50–60.
24. Goon, P. K., T. Igakura, E. Hanon, A. J. Mosley, A. Barfield, A. L. Barnard, L. Kaftantzi, Y. Tanaka, G. P. Taylor, J. N. Weber, and C. R. Bangham. 2004. Human T cell lymphotropic virus type I (HTLV-I)-specific $CD4^+$ T cells: immunodominance hierarchy and preferential infection with HTLV-I. *J. Immunol.* 172: 1735–1743.
25. Toulza, F., A. Heaps, Y. Tanaka, G. P. Taylor, and C. R. Bangham. 2008. High frequency of $CD4^+FoxP3^+$ cells in HTLV-1 infection: inverse correlation with HTLV-1-specific CTL response. *Blood* 111: 5047–5053.
26. Satou, Y., J. Yasunaga, M. Yoshida, and M. Matsuoka. 2006. HTLV-I basic leucine zipper factor gene mRNA supports proliferation of adult T cell leukemia cells. *Proc. Natl. Acad. Sci. USA* 103: 720–725.
27. Sugata, K., Y. Satou, J. Yasunaga, H. Hara, K. Ohshima, A. Utsunomiya, M. Mitsuyama, and M. Matsuoka. 2012. HTLV-1 bZIP factor impairs cell-mediated immunity by suppressing production of Th1 cytokines. *Blood* 119: 434–444.
28. Iwasaki, Y., Y. Ohara, I. Kobayashi, and S. Akizuki. 1992. Infiltration of helper/inducer T lymphocytes heralds central nervous system damage in human T-cell leukemia virus infection. *Am. J. Pathol.* 140: 1003–1008.
29. Umehara, F., S. Izumo, M. Nakagawa, A. T. Ronquillo, K. Takahashi, K. Matsumuro, E. Sato, and M. Osame. 1993. Immunocytochemical analysis of the cellular infiltrate in the spinal cord lesions in HTLV-I-associated myelopathy. *J. Neuropathol. Exp. Neurol.* 52: 424–430.
30. Umehara, F., S. Izumo, A. T. Ronquillo, K. Matsumuro, E. Sato, and M. Osame. 1994. Cytokine expression in the spinal cord lesions in HTLV-I-associated myelopathy. *J. Neuropathol. Exp. Neurol.* 53: 72–77.
31. Kurihara, K., Y. Shimizu, A. Takamori, N. Harashima, M. Noji, T. Masuda, A. Utsunomiya, J. Okamura, and M. Kannagi. 2006. Human T-cell leukemia virus type-I (HTLV-I)-specific T-cell responses detected using three-divided glutathione-*S*-transferase (GST)-Tax fusion proteins. *J. Immunol. Methods* 313: 61–73.
32. Harashima, N., R. Tanosaki, Y. Shimizu, K. Kurihara, T. Masuda, J. Okamura, and M. Kannagi. 2005. Identification of two new HLA-A*1101-restricted tax epitopes recognized by cytotoxic T lymphocytes in an adult T-cell leukemia patient after hematopoietic stem cell transplantation. *J. Virol.* 79: 10088–10092.
33. Rammensee, H. G., T. Friede, and S. Stevanoviíc. 1995. MHC ligands and peptide motifs: first listing. *Immunogenetics* 41: 178–228.
34. Hanon, E., S. Hall, G. P. Taylor, M. Saito, R. Davis, Y. Tanaka, K. Usuku, M. Osame, J. N. Weber, and C. R. Bangham. 2000. Abundant tax protein expression in $CD4^+$ T cells infected with human T-cell lymphotropic virus type I (HTLV-I) is prevented by cytotoxic T lymphocytes. *Blood* 95: 1386–1392.
35. Richardson, J. H., A. J. Edwards, J. K. Cruickshank, P. Rudge, and A. G. Dalgleish. 1990. In vivo cellular tropism of human T-cell leukemia virus type 1. *J. Virol.* 64: 5682–5687.
36. Sakai, J. A., M. Nagai, M. B. Brennan, C. A. Mora, and S. Jacobson. 2001. In vitro spontaneous lymphoproliferation in patients with human T-cell lymphotropic virus type I-associated neurologic disease: predominant expansion of $CD8^+$ T cells. *Blood* 98: 1506–1511.
37. Elovaara, I., S. Koenig, A. Y. Brewah, R. M. Woods, T. Lehky, and S. Jacobson. 1993. High human T cell lymphotropic virus type 1 (HTLV-1)-specific precursor cytotoxic T lymphocyte frequencies in patients with HTLV-1-associated neurological disease. *J. Exp. Med.* 177: 1567–1573.
38. Kannagi, M., H. Shida, H. Igarashi, K. Kuruma, H. Murai, Y. Aono, I. Maruyama, M. Osame, T. Hattori, H. Inoko, et al. 1992. Target epitope in the Tax protein of human T-cell leukemia virus type I recognized by class I major histocompatibility complex-restricted cytotoxic T cells. *J. Virol.* 66: 2928–2933.
39. Pique, C., A. Ureta-Vidal, A. Gessain, B. Chancerel, O. Gout, R. Tamouza, F. Agis, and M. C. Dokhélar. 2000. Evidence for the chronic in vivo production of human T cell leukemia virus type I Rof and Tof proteins from cytotoxic T lymphocytes directed against viral peptides. *J. Exp. Med.* 191: 567–572.
40. Sundaram, R., Y. Sun, C. M. Walker, F. A. Lemonnier, S. Jacobson, and P. T. Kaumaya. 2003. A novel multivalent human CTL peptide construct elicits robust cellular immune responses in HLA-A*0201 transgenic mice: implications for HTLV-1 vaccine design. *Vaccine* 21: 2767–2781.
41. Vollers, S. S., and L. J. Stern. 2008. Class II major histocompatibility complex tetramer staining: progress, problems, and prospects. *Immunology* 123: 305–313.
42. Sabatino, J. J., Jr., J. Huang, C. Zhu, and B. D. Evavold. 2011. High prevalence of low affinity peptide-MHC II tetramer-negative effectors during polyclonal $CD4^+$ T cell responses. *J. Exp. Med.* 208: 81–90.
43. Goulder, P. J., A. K. Sewell, D. G. Lalloo, D. A. Price, J. A. Whelan, J. Evans, G. P. Taylor, G. Luzzi, P. Giangrande, R. E. Phillips, and A. J. McMichael. 1997. Patterns of immunodominance in HIV-1-specific cytotoxic T lymphocyte responses in two human histocompatibility leukocyte antigens (HLA)-identical siblings with HLA-A*0201 are influenced by epitope mutation. *J. Exp. Med.* 185: 1423–1433.
44. Nowak, M. A., R. M. May, R. E. Phillips, S. Rowland-Jones, D. G. Lalloo, S. McAdam, P. Klenerman, B. Köppe, K. Sigmund, C. R. Bangham, et al. 1995. Antigenic oscillations and shifting immunodominance in HIV-1 infections. *Nature* 375: 606–611.
45. Goulder, P. J., M. A. Altfeld, E. S. Rosenberg, T. Nguyen, Y. Tang, R. L. Eldridge, M. M. Addo, S. He, J. S. Mukherjee, M. N. Phillips, et al. 2001. Substantial differences in specificity of HIV-specific cytotoxic T cells in acute and chronic HIV infection. *J. Exp. Med.* 193: 181–194.
46. Wherry, E. J., J. N. Blattman, K. Murali-Krishna, R. van der Most, and R. Ahmed. 2003. Viral persistence alters CD8 T-cell immunodominance and tissue distribution and results in distinct stages of functional impairment. *J. Virol.* 77: 4911–4927.
47. Jeffery, K. J., K. Usuku, S. E. Hall, W. Matsumoto, G. P. Taylor, J. Procter, M. Bunce, G. S. Ogg, K. I. Welsh, J. N. Weber, et al. 1999. HLA alleles de-

termine human T-lymphotropic virus-I (HTLV-I) proviral load and the risk of HTLV-I-associated myelopathy. *Proc. Natl. Acad. Sci. USA* 96: 3848–3853.
48. Sabouri, A. H., M. Saito, K. Usuku, S. N. Bajestan, M. Mahmoudi, M. Forughipour, Z. Sabouri, Z. Abbaspour, M. E. Goharjoo, E. Khayami, et al. 2005. Differences in viral and host genetic risk factors for development of human T-cell lymphotropic virus type 1 (HTLV-1)-associated myelopathy/tropical spastic paraparesis between Iranian and Japanese HTLV-1-infected individuals. *J. Gen. Virol.* 86: 773–781.
49. Kurihara, K., N. Harashima, S. Hanabuchi, M. Masuda, A. Utsunomiya, R. Tanosaki, M. Tomonaga, T. Ohashi, A. Hasegawa, T. Masuda, et al. 2005. Potential immunogenicity of adult T cell leukemia cells in vivo. *Int. J. Cancer* 114: 257–267.
50. Aubert, R. D., A. O. Kamphorst, S. Sarkar, V. Vezys, S. J. Ha, D. L. Barber, L. Ye, A. H. Sharpe, G. J. Freeman, and R. Ahmed. 2011. Antigen-specific CD4 T-cell help rescues exhausted CD8 T cells during chronic viral infection. *Proc. Natl. Acad. Sci. USA* 108: 21182–21187.

blood

2013 121: 4340-4347
Prepublished online March 28, 2013;
doi:10.1182/blood-2012-08-446922

Preapoptotic protease calpain-2 is frequently suppressed in adult T-cell leukemia

Makoto Ishihara, Natsumi Araya, Tomoo Sato, Ayako Tatsuguchi, Naomi Saichi, Atae Utsunomiya, Yusuke Nakamura, Hidewaki Nakagawa, Yoshihisa Yamano and Koji Ueda

Blood (print ISSN 0006-4971, online ISSN 1528-0020), is published weekly by the American Society of Hematology, 2021 L St, NW, Suite 900, Washington DC 20036.

Regular Article

LYMPHOID NEOPLASIA

Preapoptotic protease calpain-2 is frequently suppressed in adult T-cell leukemia

Makoto Ishihara,[1] Natsumi Araya,[2] Tomoo Sato,[2] Ayako Tatsuguchi,[1] Naomi Saichi,[1] Atae Utsunomiya,[3] Yusuke Nakamura,[4] Hidewaki Nakagawa,[1] Yoshihisa Yamano,[2] and Koji Ueda[1]

[1]Laboratory for Biomarker Development, Center of Genomic Medicine, RIKEN, Tokyo, Japan; [2]Department of Molecular Medical Science, Institute of Medical Science, St. Marianna University School of Medicine, Kawasaki, Japan; [3]Department of Hematology, Imamura Bun-in Hospital, Kagoshima, Japan; and [4]Section of Hematology/Oncology, Department of Medicine Faculty, The University of Chicago, Chicago, IL

Key Points

- Proteome-wide analysis of HTLV-1–infected T cells identified 17 biomarker proteins for the diagnosis of ATL or HAM/TSP patients.

Adult T-cell leukemia (ATL) is one of the most aggressive hematologic malignancies caused by human T-lymphotropic virus type 1 (HTLV-1) infection. The prognosis of ATL is extremely poor; however, effective strategies for diagnosis and treatment have not been established. To identify novel therapeutic targets and diagnostic markers for ATL, we employed focused proteomic profiling of the $CD4^+CD25^+CCR4^+$ T-cell subpopulation in which HTLV-1–infected cells were enriched. Comprehensive quantification of 14 064 peptides and subsequent 2-step statistical analysis using 29 cases (6 uninfected controls, 5 asymptomatic carriers, 9 HTLV-1–associated myelopathy/tropical spastic paraparesis patients, 9 ATL patients) identified 91 peptide determinants that statistically classified 4 clinical groups with an accuracy rate of 92.2% by cross-validation test. Among the identified 17 classifier proteins, α-II spectrin was drastically accumulated in infected T cells derived from ATL patients, whereas its digestive protease calpain-2 (CAN2) was significantly downregulated. Further cell cycle analysis and cell growth assay revealed that rescue of CAN2 activity by overexpressing constitutively active CAN2 (Δ_{19}CAN2) could induce remarkable cell death on ATL cells accompanied by reduction of α-II spectrin. These results support that proteomic profiling of HTLV-1–infected T cells could provide potential diagnostic biomarkers and an attractive resource of therapeutic targets for ATL. (*Blood*. 2013;121(21):4340-4347)

Introduction

Human T-lymphotropic virus type 1 (HTLV-1) is a human retrovirus that is the pathogenic agent of HTLV-1–associated diseases, such as adult T-cell leukemia (ATL) and HTLV-1–associated myelopathy/tropical spastic paraparesis (HAM/TSP). Recent epidemiological studies revealed that HTLV-1 is endemic mainly in Japan, the Caribbean basin, Iran, Africa, South America, and the Melanesian islands.[1] Other estimates have shown that 20 million to 30 million people worldwide are infected with HTLV-1.[2] The infection is followed by a prolonged asymptomatic phase of 20 to 30 years, and 2% to 5% of the infected individuals develop ATL during their lifetime.[3] ATL is one of the most aggressive hematologic malignancies characterized by increased numbers of lymphocytes with multilobulated nuclei, so-called flower cells, in blood circulation. The prognosis is severe with the median overall survival period and 5-year survival rate of ATL patients of 7 months and 20%, respectively.[4] Recently, humanized anti-CCR4 (KW-0761) therapeutic antibody achieved a great improvement in ATL treatment in a phase 3 study. However, the disease control rate was restricted to 50%, and long-term prognosis has yet to be known.[5] For future improvements in the management of ATL, novel biomarkers for early diagnosis are urgently needed for early therapeutic intervention.

To date, comprehensive genomic or proteomic studies using $CD4^+$ T cells have been performed for this purpose,[6-9] but reproducibility and reliability of quantification results in the discovery phase were uncertain due to the diverse individual variety of HTLV-1–infected cell contents in $CD4^+$ T cells. To overcome the etiologic variety of samples, we focused on the $CD4^+CD25^+CCR4^+$ T-cell subpopulation since Yamano et al[10] recently revealed that HTLV-1 preferentially infected $CD4^+CD25^+CCR4^+$ T cells in both ATL and HAM/TSP patients. By targeting $CD4^+CD25^+CCR4^+$ T cells, we here provide the first quantitative proteome map illustrating molecular disorders in pathogenic human T cells directly associated with the onset or progression of ATL. The comprehensive and comparative interpretation of total proteome in infected cells, especially between asymptomatic HTLV-1 carriers and ATL patients, could immediately lead to specific candidates for biomarkers and drugs.

Another challenge to emphasize in this study is our recently established proteomic profiling technologies. It is indisputable that the greater the number of clinical samples analyzed, the more confidently statistical analysis can be undertaken in order to identify diagnostic markers and druggable targets. Despite this fact, previous proteomics reports could not provide high-throughput quantitative methodologies that were sufficient for dealing with even more than 10 clinical samples, excepting a study utilizing a surface enhanced laser desorption/ionization time of flight mass spectrometer. Although the surface enhanced laser desorption/ionization time of flight method drastically improved the performance in both quantification and throughput, allowing relative quantification

Submitted August 1, 2012; accepted March 25, 2013. Prepublished online as *Blood* First Edition paper, March 28, 2013; DOI 10.1182/blood-2012-08-446922.

The online version of this article contains a data supplement.

The publication costs of this article were defrayed in part by page charge payment. Therefore, and solely to indicate this fact, this article is hereby marked "advertisement" in accordance with 18 USC section 1734.

analysis for 96 samples in several hours, at most only 250 unidentified protein peaks were detectable. In the present study, we integrated the proteomics server for the huge data set "Expressionist" (Genedata A.G., Basel, Switzerland) with high-end mass spectrometers to maximize the quality and quantity of protein catalogs transferred from mass spectrometers. We first describe the discovery phase providing a panel of novel diagnostic molecules from quantification of 14 064 peptides and identification of 4763 proteins. As the functional validation phase, we further examined the physiological potential of an identified diagnostic marker candidate, calpain-2 (CAN2), particularly concerning the association of its activity with survival or progression of ATL cells.

Materials and methods

PBMCs and cell lines

Peripheral blood mononuclear cells (PBMCs) from 6 normal donors, 5 asymptomatic carriers, and 9 HAM/TSP patients used in the screening analysis were collected in the St. Marianna University School of Medicine. Those from 9 ATL patients were collected in the Imamura Bun-in Hospital. PBMCs from 4 ATL patients used for the validation experiments were provided by the Joint Study on Predisposing Factors of ATL Development. The others from 4 HAM/TSP patients were collected in the St. Marianna University School of Medicine. The use of these human specimens in this study was approved by individual institutional ethical committees: the Ethical Committee of Yokohama Institute, RIKEN (approval code Yokohama H22-3); the Ethical Committee of St. Marianna University School of Medicine; the Institutional Review Board of Imamura Bun-in Hospital; and the Ethical Committee of the University of Tokyo (approval code 10-50). This study was conducted in accordance with the Declaration of Helsinki.

SO-4, KOB, and KK1 cells were kindly provided by Dr Yasuaki Yamada, cultured in RPMI 1640 supplemented with 10% fetal bovine serum (Cell Culture Bioscience, Tokyo, Japan), 100 kU/L interleukin 2 (Cell Science & Technology Institute Inc., Tokyo, Japan), and 1 × antibiotic-antimycotic solution (Sigma-Aldrich, MO). Jurkat, SUP-T1, CCRF-CEM, and MOLT-3 cells were cultured in RPMI 1640 supplemented with 10% fetal bovine serum and 1 × antibiotic-antimycotic solution. All cell lines were grown at 37°C in 5% CO_2. $CD3^+CD4^+CD25^+CCR4^+$ T cells were isolated with anti-CD3-FITC (eBioscience, San Diego, CA), anti-CCR4-PE (Becton Dickinson, CA), anti-CD4-Cy7 (eBioscience), and anti-CD25-APC (eBioscience) on a Cell Sorter JSAN (Bay Bioscience, Hyogo, Japan).

Sample preparation for mass spectrometric analysis

The $CD4^+CD25^+CCR4^+$ T cells were washed with phosphate-buffered saline 3 times and lysed in denaturation buffer (8 M urea in 50 mM ammonium bicarbonate). After sonication, reduction with 5 mM tris(2-carboxyethyl) phosphine (Sigma-Aldrich) at 37°C for 30 minutes, and alkylation with 25 mM iodacetamide (Sigma-Aldrich) at room temperature for 45 minutes, lysates were digested with Trypsin GOLD (Promega, WI) with protein/enzyme ratio of 25:1 at 37°C for 12 hours. The digested peptides were desalted with Oasis HLB μElution plate (Waters, MA). The collected samples were dried up with a Vacuum Spin Drier (TAITEC Co. Ltd., Saitama, Japan) and subjected to mass spectrometric analyses.

Liquid chromatography tandem mass spectrometry (LC/MS/MS)

The digested peptides were separated on a 0.1 × 200 mm homemade C_{18} column using a 2-step linear gradient, 2% to 35% acetonitrile for 95 minutes and 35% to 95% acetonitrile for 15 minutes in 0.1% formic acid with a flow rate of 200 nL/min. The eluting peptides were analyzed with a QSTAR-Elite mass spectrometer (AB Sciex, CA) in the smart information-dependent acquisition mode of Analyst QS software 2.0 (AB Sciex). The other parameters on QSTAR-Elite were shown as follows: DP = 60, FP = 265, DP2 = 15, CAD = 5, IRD = 6, IRW = 5, curtain gas = 20, and ion spray voltage = 2000 V.

Two-dimensional (2D) LC/MS/MS

Tryptic digests of $CD4^+CD25^+CCR4^+$ T cells were dissolved in 10 mM ammonium formate in 25% acetonitrile and fractionated by a 0.2 × 250 mm monolith strong cation exchange column (GL Science, Tokyo, Japan). Peptides were eluted with an ammonium formate gradient from 10 mM to 1 M in curve = 3 mode for 70 minutes using a Prominence high-performance liquid chromatography (HPLC) system (Shimadzu Corporation, Kyoto, Japan). The eluate was fractionated into 20 fractions and analyzed individually by LTQ-Orbitrap-Velos mass spectrometer (Thermo Scientific, Bremen, Germany) accompanied with the Ultimate 3000 nano-HPLC system. The fractionated peptide samples were separated with the same gradient used in the QSTAR-Elite system described previously and analyzed by LTQ-Orbitrap-Velos acquiring a full MS scan on Fourier-transition mode with MS resolution = 60 000 and simultaneously MS/MS scans for the 20 most intense precursor ions in each MS spectrum on ion-trap mode with regular resolution. Other important parameters for LTQ-Orbitrap-Velos were as follows: capillary temp = 250, source voltage = 2 kV, MS scan range = mass-to-charge ratio (m/z) 400 to 1600, acquire data dependent CID MS/MS for top-20 intense precursors, and dynamic exclusion enabled during 30 seconds. For protein identification, all MS/MS spectra were searched against SwissProt database version 2012_06 (20 232 human protein sequences) using SEQUEST algorithm on ProteomeDiscoverer 1.3 software (Thermo Scientific) with the following parameters: MS tolerance = 3 ppm, MS/MS tolerance = 0.8 Da, maximum missed cleavages = 2, enzyme = trypsin, taxonomy = *Homo sapiens*, fixed modification = carbamidomethylation on cysteine, and variable modification = oxidation on methionine. We accepted the protein identification satisfying the false discovery rate <1% by Percolator false discovery rate estimation algorithm on ProteomeDiscoverer.

Label-free quantification analysis

The LC/MS/MS raw data were imported into the Expressionist RefinerMS module and subjected to the following data processing and relative quantification steps. The total work flow on the RefinerMS module is shown in supplemental Figure 1 (see the *Blood* Web site). The LC/MS/MS raw data set from 29 clinical samples was displayed in 2D planes (m/z vs retention time [RT]). The chromatogram grid was applied to all planes: scan counts = 10, polynom order = 3, and RT smoothing = 0. The planes were simplified by subtracting background noises using chromatogram chemical noise subtraction: RT window = 50 scans, quantile subtraction = 50%, and RT smoothing = 3 scans. After the noise subtraction, data points with intensity <10 were clipped to zero. The RT variety among 29 planes was adjusted by chromatogram RT alignment: RT transformation window = 0.2 minutes, RT search interval = 5 minutes, m/z window = 0.1 Da, and gap penalty = 1. Peaks were detected by chromatogram summed peak detection: summation window = 5 scans, overlap = 50, minimum peak size = 4 scans, maximum merge distance = 10 points, peak RT splitting = true, intensity profiling = max, gap/peak ratio = 1%, refinement threshold = 5, consistency threshold = 0.8, and signal/noise threshold = 1. The detected peaks were grouped into isotopic clusters derived from each molecule using 2-step chromatogram isotopic peak clustering. The first parameters were as follows: minimum charge = 1, maximum charge = 10, maximum missing peaks = 0, first allowed gap position = 3, RT window = 0.1 minute, m/z tolerance = 0.05 Da, isotope shape tolerance = 10, and minimum cluster size ration = 1.2. The second parameters were as follows: minimum charge = 1, maximum charge = 10, maximum missing peaks = 0, first allowed gap position = 3, RT window = 0.1 minute, m/z tolerance = 0.05 Da, and minimum cluster size ration = 0.6.

Expression vectors and siRNA

For the Δ_{19}CAN2 construct, the *CAPN2* fragment was amplified with primers 5′-CATGTCGACTCCCACGAGAGGGCCATCAAGT-3′ and 5′-CATTC-TAGATCAAAGTACTGAGAAACAGAGCC-3′ from pBlueBacIII *CAPN2* and cloned into pEFBOS-Myc. Prior to the overexpression experiments, we confirmed that the sequence of the inserted *CAPN2* fragment was identical to the Mammalian Gene Collection sequence (accession number

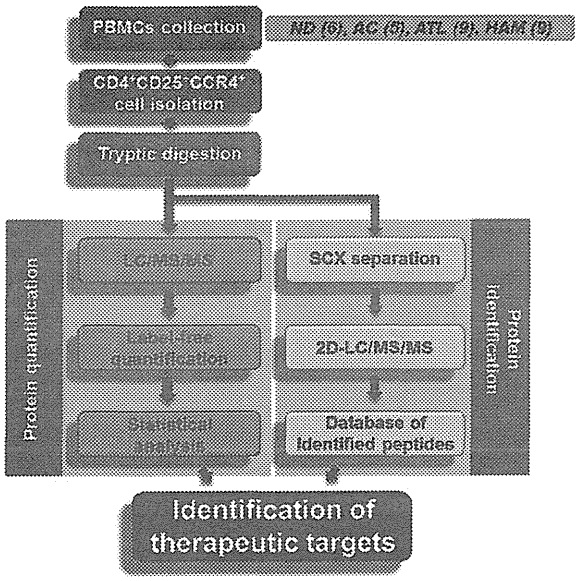

Figure 1. Schematic overview of proteomic profiling for $CD4^+CD25^+CCR4^+$ cells. PBMCs were collected from 6 normal donors, 5 asymptomatic carriers, 9 ATL patients, and 9 HAM/TSP patients, followed by isolation of the $CD4^+CD25^+CCR4^+$ subset using the cell-sorting system. The statistical candidate selection steps, including LC/MS/MS data processing, label-free quantification, and statistical analysis, were performed on the Expressionist proteome server. The protein identification database was separately established based on 2D LC/MS/MS analysis. ND, normal donors; AC, asymptomatic carriers.

BC021303). The 5-μg vector DNA was transfected to 1×10^6 cells. The small interfering RNAs (siRNAs) against *SPTAN1*, *PTMS*, *HSPE1*, and SHMT2 and siRNA universal negative control were purchased from Sigma-Aldrich. The 500-pmol siRNA oligo was transfected into 1×10^6 cells. The vectors and siRNAs were transfected into all cell lines except CCRF-CEM by Amaxa Nucleoportator transfection Kit V (Lonza, Cologne, Germany) and CCRF-CEM by Kit C (Lonza).

Cell cycle analysis and proliferation assay

For the cell cycle analysis, 1×10^5 to 2×10^5 cells were washed and agitated in 0.1% Triton-X (Sigma-Aldrich) with 100 ng/mL of ribonuclease (Sigma-Aldrich). Following addition of 1 μg/mL propidium iodide, the flow cytometric analysis was performed on FACScalibur (Becton Dickinson). The data analysis was performed using FlowJo software (Tree Star Inc., OR). Doublet events were eliminated from analyses by proper gating on FL2-W/FL2-A primary plots before histogram analysis of DNA content. Cell proliferation was estimated by measuring cell metabolic activity using Cell Counting Kit-8 (Dojindo, Kumamoto, Japan) following the manufacturer's recommendation.

Western blotting

Cells were lysed in lysis buffer [1% NP-40, 2 mM EGTA, 2 mM $MgCl_2$, 150 mM NaCl, 20 mM tris(hydroxymethyl)aminomethane–HCl (pH 7.5), 10% glycerol, containing the protease inhibitor cocktail Complete (Roche, IN)] and subjected to sodium dodecyl sulfate–polyacrylamide gel electrophoresis and transferred onto PVDF membranes. Following blocking with 4% Block Ace (Yukijirushi Nyugyo Inc., Tokyo, Japan), membranes were incubated with anti-myc (9E10; Sigma-Aldrich) or anti–α-II spectrin (Abcam, Cambridge, UK) antibodies. Membranes were then incubated with horseradish peroxidase–conjugated anti-mouse IgG (GE Healthcare, NJ) or anti-rabbit IgG (GE Healthcare), respectively, and visualized with Western Lightning kit (Perkin Elmer, MA).

Multiple reaction monitoring (MRM)

$CD4^+$ T cells were isolated from PBMCs using flow cytometry. The tryptic digests of the isolated cells were analyzed by 4000 Q-TRAP mass spectrometer (AB Sciex) accompanied with Ultimate 3000 nano-HPLC system. The LC gradient was as follows: 2% to 30% acetonitrile for 10 minutes and 30% to 95% acetonitrile for 5 minutes in 0.1% formic acid with a flow rate of 300 nL/min. The MRM transitions monitored were m/z 409.7/375.2 for α-II spectrin (SPTA2); m/z 538.3/889.5 for parathymosin (PTMS); m/z 507.3/147.1 for heat shock 10-kDa protein, mitochondrial (CH10); m/z 490.3/147.1 for serine hydroxymethyltransferase, mitochondrial (GLYM); and m/z 581.3/919.5 for β-actin, respectively. Individual peak areas were normalized by the peak area of β-actin. Data acquisition was performed with ion spray voltage = 2300 V, curtain gas = 10 psi, nebulizer gas = 10 psi, and an interface heating temperature = 150°C. The parameters were set as follows: declustering potential = 60, entrance potential = 10, collision cell exit potential = 10, and dwell time for each transition = 10 seconds. Collision energy was optimized to achieve maximum intensity for each MRM transition as follows: 34.03 V for m/z 409.7/175.1, 24.68 eV for m/z 538.3/889.5, 23.32 eV for m/z 507.3/147.1, 37.57 eV for m/z 490.3/147.1, and 31.58 eV for m/z 581.3/919.5.

Results

Quantitative proteome profiling of $CD4^+CD25^+CCR4^+$ T cells

A schematic overview of the screening approach is shown in Figure 1. To identify diagnostic markers expressed in HTLV-1–infected T cells, a $CD4^+CD25^+CCR4^+$ subset of PBMCs from 6 uninfected volunteers, 5 asymptomatic carriers, 9 HAM/TSP patients, and 9 ATL patients was isolated by flow cytometry (Figure 2). The averaged proportion of $CD4^+CD25^+CCR4^+$ cells in $CD4^+$ T cells from 4 clinical groups was 6.48 ± 2.46%, 13.17 ± 13.06%, 20.55 ± 10.73%, and 55.83 ± 22.40%, respectively, indicating that the occupancy of viral reservoir cells varied drastically among both pathological groups and even individuals within a group. Enrichment of the infected cells was confirmed by viral load measurement of the used samples (supplemental Figure 2). As reported previously,[10] the viral load of $CD4^+CD25^+CCR4^+$ cells (37.91 copies/100 cells on average) was ~10 times higher than that of $CD4^+CD25^-CCR4^-$ cells (4.12 copies/100 cells on average), indicating that the former cells were evidently the HTLV-1–enriched fraction. This fact strongly supports the importance of

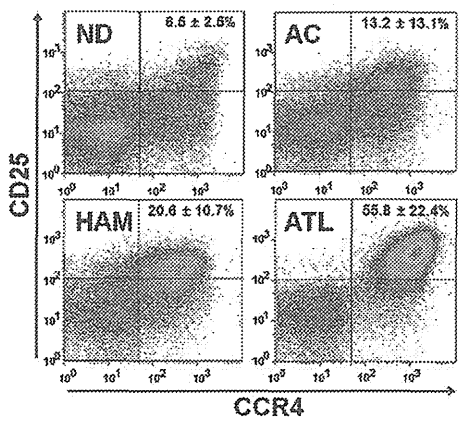

Figure 2. Representative sorting results of $CD4^+CD25^+CCR4^+$ cells. After labeling with anti-CD3-FITC, anti-CD4-Cy7, anti-CD25-APC, and anti-CCR4-PE, the $CD3^+CD4^+CD25^+CCR4^+$ fraction was isolated. The averaged content ± standard deviation (%) of $CD25^+CCR4^+$ cells out of $CD3^+CD4^+$ cells was calculated for each clinical group and is displayed in the upper right section of the panels.

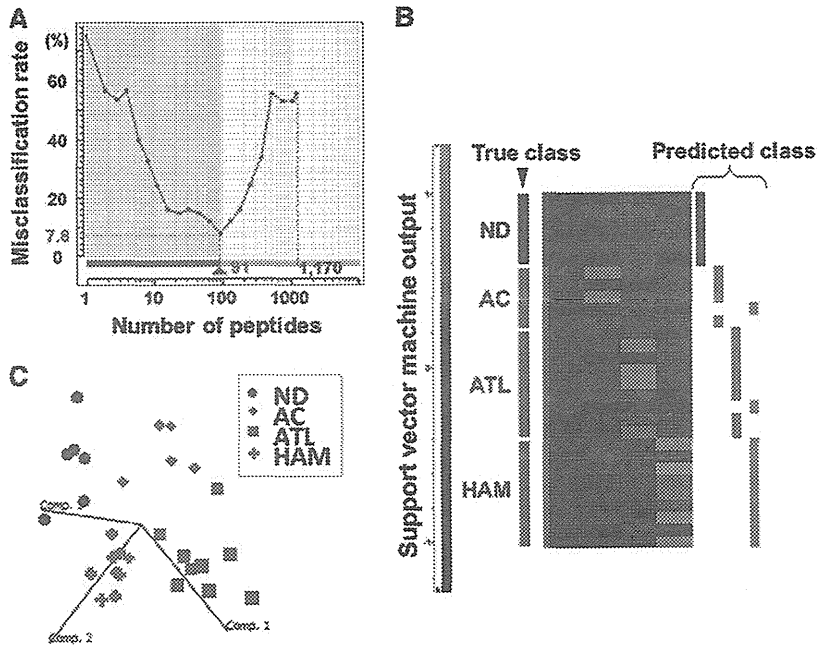

Figure 3. Statistical extraction of candidate therapeutic targets. The 14 064 nonredundant peptides detected were subjected to a 4-group Kruskal-Wallis test (ND, AC, ATL, and HAM), resulting in identification of 1170 first candidates ($P < .01$). ND, normal donors; AC, asymptomatic carriers. (A) Next, the Expressionist ranking method further narrowed down the candidates to 91 peptides based on SVM-REF so that the misclassification rate in the cross-validation test became minimum, 7.8%. (B) The predicted classification result by leave-one-out cross-validation test. The 27 out of 29 cases were successfully classified into the true classes. (C) The three-dimensional plot shows the additional assessment for the classification power of 91 classifiers by principal component analysis. Comp. 1 to 3 indicate principal components 1 to 3.

enriching pathogenic cells for rigorous quantitative biomarker discovery.

An accurately adjusted number of $CD4^+CD25^+CCR4^+$ cells from 29 cases were digested with trypsin and subjected to LC/MS/MS analysis individually. Because recent mass spectrometers often deal with data on the order of hundreds of megabytes per sample, it has been considered almost impossible to calculate a data set larger than a gigabyte from large-scale clinical samples on desktop computers. Hence, we constructed a proteomics server equipped with a 12-core central processing unit, 36 SAS hard disks, and 192-GB physical memories driving the Expressionist, which was designed to combine the database module, the data processing module, and the statistical analysis module into a single integrative platform for genomics, proteomics, and metabolomics. The detailed work flow for data processing and quantification for 29 LC/MS/MS raw data was described in the "Materials and methods" and is illustrated in supplemental Figure 1. Finally, 68 454 nonredundant peaks were detected and grouped into 37 143 isotopic clusters, or molecules. As tryptic peptides should appear as multivalent ions in electrospray ionization mass spectra, 23 079 singly charged ions were removed, resulting in utilization of 14 064 peptide signals for further statistical selection of diagnostic markers.

Statistical identification of candidate diagnostic markers for ATL

A stepwise statistical extraction was employed for the effective identification of proteins, which demonstrated specific up- or downregulation in the ATL group. In the first stage, a 4-group Kruskal-Wallis test was performed to roughly extract the candidates showing a significantly distinct expression level among 4 clinical groups. Here we set the cutoff line at $P < .01$ and obtained 1170 first candidate peptides simply because the isolated peptide set using this criterion showed the best performance in the following prediction model.

Next, we selected the final candidates by the support vector machine–recursive feature elimination algorithm in the Expressionist Analyst module. Support vector machine–recursive feature elimination is a candidate elimination method based on SVM, which enabled us to improve the classification outputs by selecting the best-performing peptide set among initially provided candidates.[11] As a result, a combination of 91 peptides showed the lowest misclassification rate (7.78%) in a leave-one-out cross-validation test (Figure 3A-B). To evaluate the classification efficiency of 91 selected candidates, the principal component analysis was performed. Figure 3C shows the three-dimensional plot of 29 clinical samples based on the 3 best-explainable components, which illustrated statistically clear segregation among the 4 clinical groups. These assessments indicated that the 91 peptides should be a sufficient set of classifiers that closely associated with the pathological characteristics of the 4 clinical groups.

Based on an independently constructed 6279-protein identification database for $CD4^+CD25^+CCR4^+$ cells using 2D LC/MS/MS (see details in "Materials and methods"), 19 peptides among the 91 candidate peptides were successfully assigned to 17 proteins listed in Table 1. The mass spectrometric quantification profiles for the 19 peptides are also shown in Figure 4 (box plots).

Recovering CAN2 activity induced cell death in ATL cells

Our diagnostic marker discovery for ATL identified an enzyme-substrate pair, CAN2 and SPTA2, which demonstrated significantly aberrant expression level in ATL patients (Figure 4). Interestingly, the intensities of the 2 proteins in 27 screening cases (without 2 statistical outliers in Figure 4) showed a clearly inverse correlation ($R^2 = 0.395$, Figure 5A). To examine whether CAN2 down-regulation and/or SPTA2 upregulation might be essential for the growth of ATL cells, the enzymatic activity of CAN2 was rescued by overexpressing the constitutively active form of CAN2 (Δ_{19}CAN2) in 3 ATL cell lines, SO-4, KOB, and KK1. After 36 hours of transfection, significant inhibition of cell proliferation (Figure 5B) and induction of sub-G1 transition was observed by activation of CAN2 in 3 ATL cells, but not in 4 non-ATL leukemia cell lines (Figure 5C). Furthermore, overexpression of Δ_{19}CAN2 drastically attenuated the expression level of SPTA2 in the ATL cell

Table 1. List of 17 protein classifiers for categorization of normal donors, asymptomatic carriers, HAM/TSP, and ATL

Accession	Protein name	*P* value (Kruskal-Wallis test)	m/z	RT	Charge	Peptide score	Identity or homology threshold	Sequence
LPPL	Eosinophil lysophospholipase	2.3.E-03	409.722	47.4	2	36.3	27	MVQVWR
CH10	Heat shock 10-kDa protein, mitochondrial	2.5.E-03	430.721	40.6	2	26.2	21	GGIMLPEK
PRG2	Bone marrow proteoglycan	2.4.E-03	528.271	64.6	2	31.6	28	RLPFICSY
MOES	Moesin	8.1.E-04	532.253	26.8	2	46.2	29	EKEELMER
MNDA	Myeloid cell nuclear differentiation antigen	9.4.E-03	647.863	69.1	2	67.3	24	SLLAYDLGLTTK
GLYM	Serine hydroxymethyltransferase, mitochondrial	8.7.E-04	408.551	21.6	3	31.1	18	HADIVTTTTHK
PTMS	Parathymosin	9.7.E-04	453.875	17.8	3	41.2	25	AAEEEDEADPKR
TPIS	Triosephosphate isomerase	9.1.E-03	472.266	71.0	3	54.0	28	QSLGELIGTLNAAK
HSP71	Heat shock 70-kDa protein 1A/1B	9.7.E-03	563.307	65.5	3	93.8	21	IINEPTAAAIAYGLDR
CD6	T-cell differentiation antigen CD6	7.7.E-03	592.306	37.8	3	62.7	22	VLCQSLGCGTAVERPK
ANXA1	Annexin A1	4.4.E-04	612.347	61.5	3	57.0	17	RKGTDVNVFNTILTTR
ANXA6	Annexin A6	2.3.E-03	669.017	70.9	3	54.7	16	AMEGAGTDEKALIEILATR
SPTA2	Spectrin α chain, brain	5.4.E-03	409.718	28.8	2	42.7	30	EAGSVSLR
GLYM	Serine hydroxymethyltransferase, mitochondrial	1.1.E-03	428.240	57.0	2	42.8	27	SGLIFYR
DRB1s	HLA class II histocompatibility antigen, DRB1-1, 4, 10, 11, 13, 15, 16 β chain	1.0.E-02	478.216	25.8	2	55.9	25	AAVDTYCR
CAN2	Calpain-2 catalytic subunit	2.4.E-03	483.253	54.0	2	66.6	29	SDTFINLR
STAT1	Signal transducer and activator of transcription 1-α/β	7.3.E-03	486.290	21.7	2	39.1	29	KILENAQR
PRG2	Bone marrow proteoglycan	9.4.E-04	497.742	49.2	2	31.6	27	FQWVDGSR
CXCL7	Platelet basic protein	1.3.E-03	528.761	43.1	2	51.7	28	ICLDPDAPR

line SO-4 (Figure 5D), but not in the non-ATL leukemia cell line Jurkat (Figure 5E). On the other hand, an additional cell proliferation assay using siRNA against *SPTAN1* revealed that reduction of SPTA2 was not sufficient for the induction of cell death for ATL cells (supplemental Figures 3 and 4).

In addition, 3 proteins (PTMS, CH10, and GLYM) were also found to be upregulated in ATL cells. To address the roles of these proteins, a cell proliferation assay was conducted using 3 ATL cell lines treated with siRNAs against *PTMS*, *HSPE1* (gene symbol of CH10), or *SHMT2* (gene symbol of GLYM) (supplemental Figure 4). As a result, suppression of the *SHMT2* gene induced significant growth inhibition for all 3 ATL cell lines. Although si*HSPE1*-treated KOB cells showed a statistically significant decrease in cell growth rate, si*HSPE1* and si*PTMS* had only partial

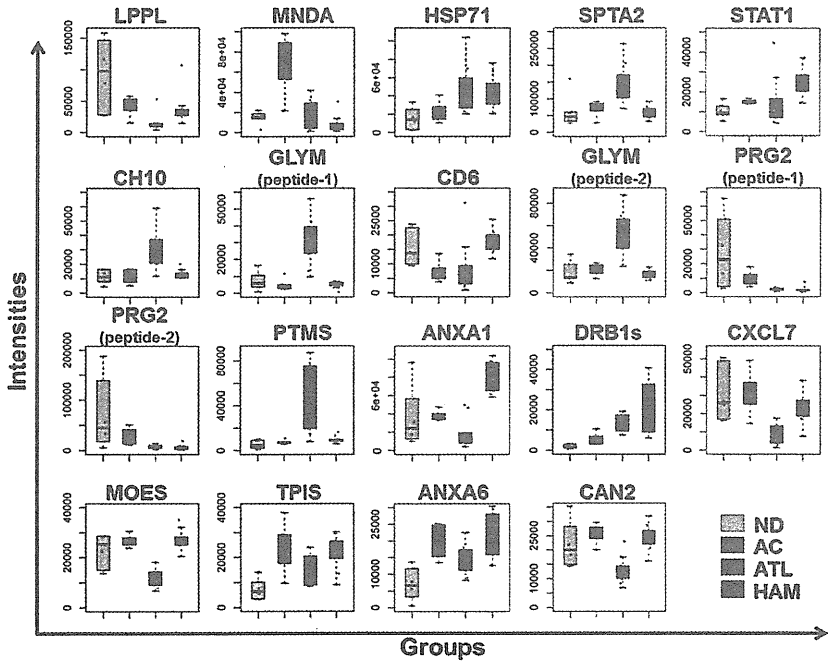

Figure 4. Summary of quantitative features for the 17 protein classifiers identified. The 19 box plots (see Table 1 for protein names) show the results of mass spectrometric quantification and protein identification. We finally identified 19 peptides out of 91 candidates in Figure 3, which were assigned to 17 proteins. Proteins identified from 2 distinct peptides were shown as GLYM (peptides 1 and 2) or PRG2 (peptides 1 and 2). The y-axis indicates normalized relative intensity of peptides in mass spectrometric data. ND, normal donors; AC, asymptomatic carriers.

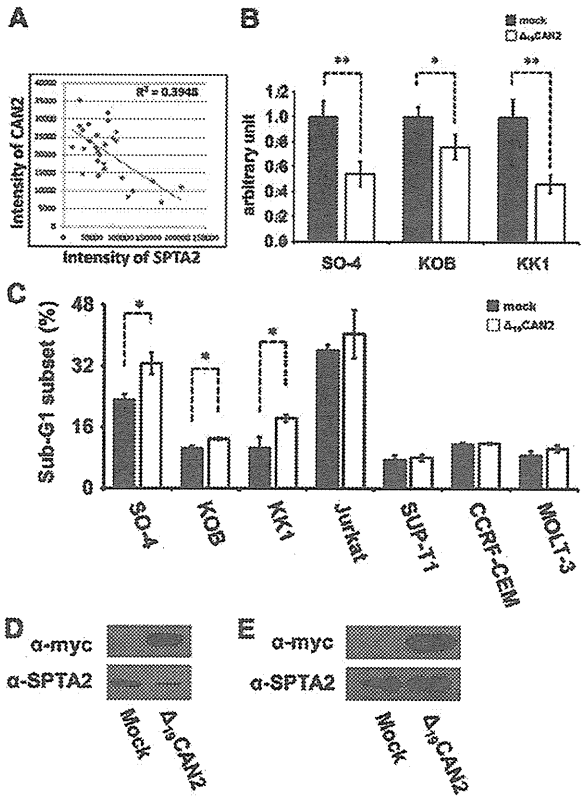

Figure 5. Rescue of CAN2 activity induced cell death in ATL cells. (A) Correlation between CAN2 and SPTA2 expression level in 27 cases. (B) Cell proliferation was measured by MTT assay on SO-4, KOB, and KK1 cells 36 hours after transfection of mock vector or Δ_{19}CAN2. $^{*}P < .05$; $^{**}P < .01$ by Student *t* test. (C) Overexpression of Δ_{19}CAN2 significantly accelerated cell death in 3 ATL (SO-4, KOB, and KK1) and 4 non-ATL (Jurkat, SUP-T1, CCRF-CEM, and MOLT-3) cell lines. $^{**}P < .05$ by Student *t* test. The drastic attenuation of SPTA2 expression was observed after transfection of Δ_{19}CAN2 in SO-4 cells (D), but not in Jurkat cells (E). The immunoblot of anti-myc tag confirmed the expression of exogenous Δ_{19}CAN2.

or no effects on proliferation of ATL cell lines. To further confirm whether the overexpression of SPTA2, PTMS, CH10, or GLYM protein would be an ATL-specific molecular signature, the expression levels of these proteins in 8 clinical samples were evaluated by the mass spectrometric quantification technology MRM (supplemental Figures 5 and 6). Expression of SPTA2, GLYM, and CH10 in cells derived from ATL patients was significantly higher than that in cells derived from HAM/TSP patients. The level of PTMS also showed a clearly increasing tendency in the ATL patient group. Taken together, these results suggested that the deprivation of CAN2 activity and upregulation of GLYM in HTLV-1–infected T cells might have a key role at the onset or progression of ATL.

Discussion

In the past decade, proteomics technologies have developed dramatically for the purpose of obtaining more and more comprehensive and sensitive proteome maps in cells or clinical specimens. The performance of mass spectrometers in particular has exhibited remarkable progress; however, as for sensitivity and throughput, it has still been difficult to identify biomarkers from crude samples including body fluids or total cell lysate. A major reason could be that the range of protein concentration in the analyte is indeed much larger than the dynamic range of recent mass spectrometers.[12] The other essential factor to be improved for clinical proteomics is the capacity of the bioinformatics platform to allow analysis of a sufficient number of clinical samples in order to statistically overcome the significant individual variability.[13]

Concerning the first issue, we previously developed and applied various focused proteomic applications targeting molecular biochemical features including glycan structure biomarkers[14-16] and low-molecular-weight peptide biomarkers.[17] The preenrichment of subproteome fractions effectively reduces the complexity of crude samples and allowed us to identify potential serum cancer biomarkers successfully. Through our previous knowledge, we provide an approach for investigating infectious diseases by employing virus-infected cell-focused proteomics. In addition to HTLV-1, for instance, isolation of HIV-infected cells is highly desired because the frequency of these cells in AIDS patients' PBMCs is ~1 out of 10^4 to 10^5 cells.[18] Actually, we successfully demonstrated the effect of HTLV-1–infected cell isolation on the elimination of individual variability (Figure 2, supplemental Figure 2) and reliable identification of disease state–associated proteins (Figures 4 and 5). We further showed the potential of the next-generation bioinformatics platform Expressionist to remove the constraint on the capacity of data size acquired from high-end mass spectrometers. Expressionist covered whole discovery steps from processing of raw mass spectrometer data to statistical analyses (Figures 1 and 3, and supplemental Figure 1) and, importantly, could perform quantification analysis using a basically unlimited number of clinical samples. Hence, in parallel with the development of mass spectrometers, high-specification and inexpensive OMICS server systems are necessary for future diagnostic marker and therapeutic target discoveries using hundreds or thousands of clinical specimens.

In this study, we focused on the $CD4^+CD25^+CCR4^+$ T-cell subpopulation in which T helper 2, T helper 17, and regulatory T (Treg) cells were mainly involved.[10] The purpose for which we used this subset was to technically enrich the preferential viral reservoir cells and to strengthen reliability of screening results. However, investigating proteome behaviors of these subtypes in HTLV-1–associated diseases is also important physiologically because it has been frequently reported that deregulated Treg plays significant roles in pathogenesis of ATL and HAM/TSP. Indeed, aberrant proliferation of Treg cells is considered the main cause of immunodeficiency in ATL patients because of their innate immunosuppressive functions,[19] whereas abnormal production of interferon γ from infected Treg cells might induce chronic spinal inflammation in HAM/TSP patients.[20] Given the list of our 17 classifier proteins, activation of signal transducer and activator of transcription 1-α/β is the well-known key factor for HAM/TSP,[21] whereas upregulation of heat shock 70-kDa protein 1A/1B, CH10, and PTMS were reported in many other types of tumors.[22-24] The association of these 4 proteins with the etiology of HAM/TSP and ATL would be evident according to the previous work, supporting that our other candidates might similarly have a direct impact on the transformation of Treg cells after infection of HTLV-1. Particularly, the specific upregulation of GLYM in ATL cells represents the first evidence that excessive folate metabolism might be essential for the progression or survival of ATL cells because GLYM is a fundamental enzyme catalyzing the supply of glycine accompanying the conversion of tetrahydrofolate to 5,10-methylenetetrahydrofolate.[25] Indeed, the suppression of GLYM expression, which was confirmed to be upregulated in ATL patients, resulted in significant reduction of cell growth. This observation suggests that diminishing GLYM

expression or enzyme activity could be a promising strategy for molecular-targeting treatment of ATL. Together with the down-regulation of CAN2 in the ATL cells shown in Figure 5, the proteins listed in Table 1 could provide the molecular basis for not only interpretation of physiological mechanisms in ATL or HAM/TSP but also development of novel therapeutic agents for HTLV-1–associated diseases.

CAN2 belongs to a Ca^{2+}-regulated cytosolic cysteine protease family, which includes 14 calpain isoforms.[26] The enzymatic activity of calpain is implicated in diverse physiological processes, such as cytoskeletal remodeling, cellular signaling, and apoptosis.[26] As an example of a spectrin-mediated apoptosis pathway, it was reported that CAN2 produced SPTA2 breakdown products following traumatic brain injury.[27] Because SPTA2 interacts with calmodulin and constructs the membrane cytoskeletons, its breakdown is considered a process of membrane structural changes during cell death.[28,29] This fact is concordant with our finding in ATL, suggesting that accumulation of SPTA2 in ATL cells can be attributed to the suppression of CAN2 expression and contribute to circumvent apoptosis. In the analysis of basal levels of CAN2 and SPTA2 in 7 cell lines (supplemental Figure 7), 3 ATL cell lines showed endogenous expression of CAN2 and moderate levels of SPTA2. On the other hand, 4 non-ATL leukemia cells demonstrated very high expression of SPTA2 and undetectable levels of CAN2. Although we found the downregulation of CAN2 and accumulation of SPTA2 in ATL cells, this tendency might be more distinctive in HTLV-1 (–) leukemia cells. Taken together, even though the expression level of CAN2 was indeed suppressed in ATL cells, the CAN2-SPTA2 apoptotic pathway itself might remain normal. In contrast, this pathway was considered to be impaired at multiple stages in HTLV-1 (–) leukemia cells because CAN2 expression was completely diminished (supplemental Figure 7) and overexpression of CAN2 could not reactivate the CAN2-SPTA2 apoptotic pathway (Figure 5B-E). In these cells, not only genetic downregulation of CAN2 but also inhibition of CAN2 enzymatic activity might be involved in the carcinogenesis.

In conclusion, comprehensive proteomic profiling of HTLV-1–infected T cells provided 17 disease-associated signature proteins, which have great potential for future clinical use as diagnostic biomarkers. As we described regarding the relationship between the CAN2-SPTA2 pathway and ATL phenotypes, further individual functional analyses will contribute to understanding the detailed molecular mechanisms involved in the onset or progression of HAM/TSP and ATL.

Acknowledgments

The authors thank Dr Hiroyuki Sorimachi for kindly providing pBlueBacIIICAPN2 vector.

This work was supported by Research on Measures for Intractable Diseases, the Ministry of Health Labour and Welfare Japan.

Authorship

Contribution: M.I. and K.U. designed the study, performed experiments, analyzed results, and wrote the manuscript; A.T. and N.S. performed experiments; N.A., T.S., A.U., and Y.Y. collected the clinical samples and performed flow cytometric experiments; Y.N. and H.N. revised the manuscript; and all authors discussed the results and commented on the manuscript.

Conflict-of-interest disclosure: The authors declare no competing financial interests.

Correspondence: Koji Ueda, Laboratory for Biomarker Development, Center for Genomic Medicine, RIKEN, General Research Building 6F, Institute of Medical Science, 4-6-1 Shirokanedai, Minato-ku, Tokyo, Japan, 1088639; e-mail: k-ueda@riken.jp.

References

1. Yamashita M, Ido E, Miura T, Hayami M. Molecular epidemiology of HTLV-I in the world. *J Acquir Immune Defic Syndr Hum Retrovirol.* 1996;13(suppl 1):S124-S131.
2. Asquith B, Zhang Y, Mosley AJ, et al. In vivo T lymphocyte dynamics in humans and the impact of human T-lymphotropic virus 1 infection. *Proc Natl Acad Sci U S A.* 2007;104(19):8035-8040.
3. Sakashita A, Hattori T, Miller CW, et al. Mutations of the p53 gene in adult T-cell leukemia. *Blood.* 1992;79(2):477-480.
4. Beltran B, Quiñones P, Morales D, Cotrina E, Castillo JJ. Different prognostic factors for survival in acute and lymphomatous adult T-cell leukemia/lymphoma. *Leuk Res.* 2011;35(3):334-339.
5. Ishida T, Joh T, Uike N, et al. Defucosylated anti-CCR4 monoclonal antibody (KW-0761) for relapsed adult T-cell leukemia-lymphoma: a multicenter phase II study. *J Clin Oncol.* 2012; 30(8):837-842.
6. Semmes OJ, Cazares LH, Ward MD, et al. Discrete serum protein signatures discriminate between human retrovirus-associated hematologic and neurologic disease. *Leukemia.* 2005;19(7):1229-1238.
7. Kirk PD, Witkover A, Courtney A, et al. Plasma proteome analysis in HTLV-1-associated myelopathy/tropical spastic paraparesis. *Retrovirology.* 2011;8:81.
8. Rahman S, Quann K, Pandya D, Singh S, Khan ZK, Jain P. HTLV-1 Tax mediated downregulation of miRNAs associated with chromatin remodeling factors in T cells with stably integrated viral promoter. *PLoS ONE.* 2012;7(4):e34490.
9. Polakowski N, Gregory H, Mesnard JM, Lemasson I. Expression of a protein involved in bone resorption, Dkk1, is activated by HTLV-1 bZIP factor through its activation domain. *Retrovirology.* 2010;7:61.
10. Yamano Y, Araya N, Sato T, et al. Abnormally high levels of virus-infected IFN-gamma+ CCR4+ CD4+ CD25+ T cells in a retrovirus-associated neuroinflammatory disorder. *PLoS ONE.* 2009;4(8):e6517.
11. Oh JH, Gao J, Nandi A, Gurnani P, Knowles L, Schorge J. Diagnosis of early relapse in ovarian cancer using serum proteomic profiling. *Genome Inform.* 2005;16(2):195-204.
12. Anderson NL, Anderson NG. The human plasma proteome: history, character, and diagnostic prospects. *Mol Cell Proteomics.* 2002;1(11): 845-867.
13. Nordon IM, Brar R, Hinchliffe RJ, Cockerill G, Thompson MM. Proteomics and pitfalls in the search for potential biomarkers of abdominal aortic aneurysms. *Vascular.* 2010;18(5):264-268.
14. Ueda K, Katagiri T, Shimada T, et al. Comparative profiling of serum glycoproteome by sequential purification of glycoproteins and 2-nitrobenzensulfenyl (NBS) stable isotope labeling: a new approach for the novel biomarker discovery for cancer. *J Proteome Res.* 2007;6(9): 3475-3483.
15. Ueda K, Fukase Y, Katagiri T, et al. Targeted serum glycoproteomics for the discovery of lung cancer-associated glycosylation disorders using lectin-coupled ProteinChip arrays. *Proteomics.* 2009;9(8):2182-2192.
16. Ueda K, Takami S, Saichi N, et al. Development of serum glycoproteomic profiling technique; simultaneous identification of glycosylation sites and site-specific quantification of glycan structure changes. *Mol Cell Proteomics.* 2010;9(9): 1819-1828.
17. Ueda K, Saichi N, Takami S, et al. A comprehensive peptidome profiling technology for the identification of early detection biomarkers for lung adenocarcinoma. *PLoS ONE.* 2011;6(4): e18567.
18. Bahbouhi B, al-Harthi L. Enriching for HIV-infected cells using anti-gp41 antibodies indirectly conjugated to magnetic microbeads. *Biotechniques.* 2004;36(1): 139-147.
19. Matsubar Y, Hori T, Morita R, Sakaguchi S, Uchiyama T. Delineation of immunoregulatory properties of adult T-cell leukemia cells. *Int J Hematol.* 2006;84(1):63-69.
20. Best I, López G, Verdonck K, et al. IFN-gamma production in response to Tax 161-233, and frequency of CD4+ Foxp3+ and Lin HLA-

DRhigh CD123+ cells, discriminate HAM/TSP patients from asymptomatic HTLV-1-carriers in a Peruvian population. *Immunology.* 2009; 128(1, pt 2):e777-e786.

21. Nakamura N, Fujii M, Tsukahara T, et al. Human T-cell leukemia virus type 1 Tax protein induces the expression of STAT1 and STAT5 genes in T-cells. *Oncogene.* 1999;18(17): 2667-2675.
22. Alaiya AA, Al-Mohanna M, Aslam M, et al. Proteomics-based signature for human benign prostate hyperplasia and prostate adenocarcinoma. *Int J Oncol.* 2011;38(4): 1047-1057.
23. Cappello F, Rappa F, David S, Anzalone R, Zummo G. Immunohistochemical evaluation of PCNA, p53, HSP60, HSP10 and MUC-2 presence and expression in prostate carcinogenesis. *Anticancer Res.* 2003;23(2B): 1325-1331.
24. Letsas KP, Vartholomatos G, Tsepi C, Tsatsoulis A, Frangou-Lazaridis M. Fine-needle aspiration biopsy-RT-PCR expression analysis of prothymosin alpha and parathymosin in thyroid: novel proliferation markers? *Neoplasma.* 2007; 54(1):57-62.
25. Anderson DD, Quintero CM, Stover PJ. Identification of a de novo thymidylate biosynthesis pathway in mammalian mitochondria. *Proc Natl Acad Sci USA.* 2011;108(37): 15163-15168.
26. Storr SJ, Carragher NO, Frame MC, Parr T, Martin SG. The calpain system and cancer. *Nat Rev Cancer.* 2011;11(5):364-374.
27. Liu MC, Akle V, Zheng W, et al. Comparing calpain- and caspase-3-mediated degradation patterns in traumatic brain injury by differential proteome analysis. *Biochem J.* 2006;394(pt 3): 715-725.
28. Wallis CJ, Wenegieme EF, Babitch JA. Characterization of calcium binding to brain spectrin. *J Biol Chem.* 1992;267(7): 4333-4337.
29. Liu X, Van Vleet T, Schnellmann RG. The role of calpain in oncotic cell death. *Annu Rev Pharmacol Toxicol.* 2004;44: 349-370.

THE JOURNAL OF IMMUNOLOGY

HTLV-1 bZIP Factor–Specific CD4 T Cell Responses in Adult T Cell Leukemia/Lymphoma Patients After Allogeneic Hematopoietic Stem Cell Transplantation

Tomoko Narita, Takashi Ishida, Ayako Masaki, Susumu Suzuki, Asahi Ito, Fumiko Mori, Tomiko Yamada, Masaki Ri, Shigeru Kusumoto, Hirokazu Komatsu, Yasuhiko Miyazaki, Yoshifusa Takatsuka, Atae Utsunomiya, Akio Niimi, Shinsuke Iida and Ryuzo Ueda

J Immunol published online 20 December 2013
http://www.jimmunol.org/content/early/2013/12/20/jimmunol.1301952

The Journal of Immunology is published twice each month by The American Association of Immunologists, Inc., 9650 Rockville Pike, Bethesda, MD 20814-3994.

Print ISSN: 0022-1767 Online ISSN: 1550-6606.

Published December 20, 2013, doi:10.4049/jimmunol.1301952

HTLV-1 bZIP Factor–Specific CD4 T Cell Responses in Adult T Cell Leukemia/Lymphoma Patients After Allogeneic Hematopoietic Stem Cell Transplantation

Tomoko Narita,* Takashi Ishida,* Ayako Masaki,* Susumu Suzuki,*,† Asahi Ito,* Fumiko Mori,* Tomiko Yamada,* Masaki Ri,* Shigeru Kusumoto,* Hirokazu Komatsu,* Yasuhiko Miyazaki,‡ Yoshifusa Takatsuka,§ Atae Utsunomiya,§ Akio Niimi,* Shinsuke Iida,* and Ryuzo Ueda†

We document human T lymphotropic virus type 1 (HTLV-1) bZIP factor (HBZ)-specific CD4 T cell responses in an adult T cell leukemia/lymphoma (ATL) patient after allogeneic hematopoietic stem cell transplantation (HCT) and identified a novel HLA-DRB1*15:01–restricted HBZ-derived naturally presented minimum epitope sequence, RRRAEKKAADVA (HBZ114–125). This peptide was also presented on HLA-DRB1*15:02, recognized by CD4 T cells. Notably, HBZ-specific CD4 T cell responses were only observed in ATL patients after allogeneic HCT (4 of 9 patients) and not in nontransplanted ATL patients (0 of 10 patients) or in asymptomatic HTLV-1 carriers (0 of 10 carriers). In addition, in one acute-type patient, HBZ-specific CD4 T cell responses were absent in complete remission before HCT, but they became detectable after allogeneic HCT. We surmise that HTLV-1 transmission from mothers to infants through breast milk in early life induces tolerance to HBZ and results in insufficient HBZ-specific T cell responses in HTLV-1 asymptomatic carriers or ATL patients. In contrast, after allogeneic HCT, the reconstituted immune system from donor-derived cells can recognize virus protein HBZ as foreign, and HBZ-specific immune responses are provoked that contribute to the graft-versus-HTLV-1 effect. *The Journal of Immunology*, **2014, 192: 000–000.**

Adult T cell leukemia/lymphoma (ATL) is a distinct hematologic malignancy caused by human T lymphotropic virus type 1 (HTLV-1) (1, 2). ATL is resistant to conventional chemotherapeutic agents, and only limited treatment options are available (3). Although early efforts using myeloablative chemoradiotherapy together with autologous hematopoietic stem cell rescue for ATL were associated with a high incidence of relapse and fatal toxicities (4), allogeneic hematopoietic stem cell transplantation (HCT) has been explored as a promising alternative treatment, achieving long-term remission in a proportion of patients with ATL (5, 6). The potential benefit of allogeneic HCT for ATL patients is considered to be due to the high immunogenicity of HTLV-1–infected cells (7–12), which was associated with the existence of posttransplant graft-versus-HTLV-1 and/or graft-versus-ATL effects (13, 14).

HTLV-1 was the first retrovirus to be directly associated with a human malignancy (15, 16), and ~20 million people worldwide are estimated to be infected with this virus (17). Among the HTLV-1 regulatory and accessory genes, *Tax* transforms rodent cells and immortalizes human primary T cells (18–20). In addition, Tax-transgenic mice develop spontaneous tumors (21–24). Another HTLV-1 component gene, *HBZ*, promotes the proliferation of ATL cells (25). Transgenic mice expressing HTLV-1 bZIP factor (HBZ) in their CD4 T cells share many symptoms and immunological features with HTLV-1–infected humans (26). Thus, both *Tax* and *HBZ* are thought to play critical roles in ATL oncogenesis, but there is a marked contrast between them in their expression profiles in primary ATL cells: HBZ expression is constitutive whereas Tax expression is frequently suppressed or minimal in ATL cells (25, 27, 28). Because immune responses against Tax were reported to be strong (7, 8), impaired Tax expression is thought to lead to a survival advantage for HTLV-1–infected cells in the host (2). These observations raise a simple question as to why the expression of Tax, but not HBZ, is impaired, despite both being HTLV-1–derived Ags seen by the human immune system as foreign. In other words, why is it that only HBZ, but not Tax, is constitutively expressed in ATL cells, although it was reported that HBZ is an immunogenic protein recognized by HBZ-specific CTL clones (29, 30). Although several studies (29–31) have been performed to determine the immunogenicity of HBZ, the precise immunological significance of HBZ in HTLV-1–infected individuals has not been fully established. Therefore, the aim of the current study was to clarify the clinical role of HBZ-specific immune responses in HTLV-1–infected individuals.

*Department of Medical Oncology and Immunology, Nagoya City University Graduate School of Medical Sciences, Nagoya 467-8601, Japan; †Department of Tumor Immunology, Aichi Medical University School of Medicine, Aichi 480-1195, Japan; ‡Department of Hematology, Oita Prefectural Hospital, Oita 870-8511, Japan; and §Department of Hematology, Imamura Bun-in Hospital, Kagoshima 890-0064, Japan

Received for publication July 22, 2013. Accepted for publication November 20, 2013.

This work was supported by grants-in-aid for scientific research (B) (No. 25290058) and scientific support programs for cancer research (No. 221S0001) from the Ministry of Education, Culture, Sports, Science and Technology of Japan, grants-in-aid from the National Cancer Center Research and Development Fund (No. 21-6-3), and H23- Third-Term Comprehensive Control Research for Cancer-general-011 from the Ministry of Health, Labour and Welfare, Japan (all to T.I.). Nagoya City University Graduate School of Medical Sciences received research grant support from Kyowa Hakko Kirin for research carried out by T.I.

Address correspondence and reprint requests to Dr. Takashi Ishida, Department of Medical Oncology and Immunology, Nagoya City University Graduate School of Medical Sciences, 1 Kawasumi, Mizuho-chou, Mizuho-ku, Nagoya, Aichi 467-8601, Japan. E-mail address: itakashi@med.nagoya-cu.ac.jp

Abbreviations used in this article: AC, asymptomatic carrier; ATL, adult T cell leukemia/lymphoma; CR, complete remission; HAM, human T lymphotropic virus type 1–associated myelopathy; HBZ, human T lymphotropic virus type 1 bZIP factor; HCT, hematopoietic stem cell transplantation; HTLV-1, human T lymphotropic virus type 1.

www.jimmunol.org/cgi/doi/10.4049/jimmunol.1301952

Materials and Methods

Primary human cells

Blood samples were obtained from healthy volunteers, HTLV-1 asymptomatic carriers (ACs), and ATL patients. Mononuclear cells were isolated with Ficoll-Paque (Pharmacia, Peapack, NJ). Genotyping of HLA-DR, HLA-DQ, and HLA-DP was performed using an WAKFlow HLA-typing kit (WAKUNAGA Pharmacy, Hiroshima, Japan). Diagnosis and classification of clinical subtypes of ATL were according to the criteria proposed by the Japan Lymphoma Study Group (32). All donors provided informed written consent before sampling, according to the Declaration of Helsinki, and the current study was approved by the institutional ethics committees of Nagoya City University Graduate School of Medical Sciences.

Cell lines

ATN-1, MT-1, TL-Om1, and ATL102 are ATL cell lines; MT-2, MT-4, and TL-Su are HTLV-1–immortalized lines; and K562 is a chronic myelogenous leukemia blast crisis cell line (8, 33). Genotyping of HLA-DR, HLA-DQ, and HAL-DP was performed using a WAKFlow HLA-typing kit.

Expansion of HBZ-specific T cells

PBMCs from ATL patients or HTLV-1 ACs were suspended in RPMI 1640 (Cell Science and Technology Institute, Sendai, Japan) supplemented with 10% human serum and 10 μM synthetic HBZ-derived peptides at a cell concentration of 2×10^6/ml. The peptides were purchased from Invitrogen (Carlsbad, CA). The cell suspension (2×10^6 cells) was cultured at 37°C in 5% CO_2 for 2 d, and an equal volume of RPMI 1640 supplemented with 100 IU/ml IL-2 was added. After subsequent culture for 5 d, an equal volume of ALyS505N (Cell Science and Technology Institute) supplemented with 100 IU/ml IL-2 was added, and the cells were cultured with appropriate medium (ALyS505N with 100 IU/ml IL-2) for an additional 7 d.

Abs and flow cytometry

PerCP-conjugated anti-CD8 mAb (SK1; eBioscience, San Diego, CA) and PE-conjugated anti-CD4 mAb [SFCI12T4D11 (T4); Beckman Coulter, Fullerton, CA] were used. For assessing HLA class II expression, PE-conjugated anti–HLA-DR (G46-6; BD Biosciences, San Jose, CA), anti–HLA-DQ (HLA-DQ1; BioLegend, San Diego, CA), or appropriate isotype-control mAbs were used. For intracellular IFN-γ and TNF-α staining, the expanded cells were cocultured with or without target cells or synthetic peptides at 37°C in 5% CO_2 for 3 h, after which brefeldin A (BD Biosciences) was added at 2 μg/ml. The cells were then incubated for an additional 2 h. Subsequently, they were fixed in 10% formaldehyde and stained with FITC-conjugated anti–IFN-γ (45.15; Beckman Coulter) or allophycocyanin-conjugated anti–TNF-α (MAb11; eBioscience) mAbs with 0.25% saponin for 60 min at room temperature. To determine HLA restriction, HLA-blocking experiments were conducted. The expanded cells were preincubated with 20 μg/ml anti–HLA-DR (L243; BioLegend), 20 μg/ml anti–HLA-DQ (1SPVL3; Beckman Coulter), or appropriate isotype control mAbs (20 μg/ml) at 37°C in 5% CO_2 for 1 h, after which they were stimulated with the peptide or the cell lines (ATN-1 and K562). Cells were analyzed on a FACSCalibur (BD Biosciences) with the aid of FlowJo software (Tree Star, Ashland, OR).

Quantitative RT-PCR

Total RNA was isolated with RNeasy Mini Kits (QIAGEN, Tokyo, Japan). Reverse transcription from the RNA to first-strand cDNA was carried out using High Capacity RNA-to-cDNA Kits (Applied Biosystems, Foster City, CA). *HBZ* and *β-actin* mRNA were amplified using TaqMan Gene Expression Assays with the aid of an Applied Biosystems StepOnePlus. The primer set for *HBZ* was as follows: sense, 5′-TCGACCTGAGCTTTAAACTTACCTAGA-3′ and antisense, 5′-GACACAGGCAAGCATCGAAA-3′. All values given are means of triplicate determinations.

Results

T cell responses against synthetic peptides overlapping by 10 aa and covering the entire sequence of the spliced HBZ protein

Because it was reported that HTLV-1 Tax-specific T cells were induced in some ATL patients after allogeneic HCT (10, 11), we initially tried to expand HBZ-specific T cells using PBMCs from an ATL patient who received allogeneic HCT with reduced-intensity conditioning and has been in complete remission (CR) for >3 y (patient #1 after HCT). PBMCs were stimulated with a mixture of 1 16-mer and 19 20-mer synthetic peptides overlapping by 10 aa and covering the entire sequence of the spliced HBZ protein (peptides number 1–20, Fig. 1), at a concentration of 10 μM each. The expanded cells were analyzed by forward scatter height and side scatter height levels, and the lymphocyte population was determined and plotted to show CD4 and CD8 positivity (Fig. 2A, *left panels*). The expanded CD8 T cells responded weakly to stimulation with these 20 overlapping peptides relative to controls without peptide stimulation, as assessed by IFN-γ production (Fig. 2A, *upper middle panels*) but not TNF-α (Fig. 2A, *lower middle panels*). In contrast, the expanded CD4 T cells responded to stimulation by the 20 overlapping peptides by producing both IFN-γ (Fig. 2A, *upper right panels*) and TNF-α (Fig. 2A, *lower right panels*). Because the response of the stimulated and expanded CD4 T cells was stronger than the CD8 response, we focused on the CD4 T cell response against HBZ in patient #1 after HCT.

PBMCs from this patient (#1 after HCT) were stimulated with a mixture of five overlapping peptides consisting of peptides 1–4, 5–8, 9–12, 13–16, and 17–20 (Fig. 1). The expanded CD4 T cells responded to the peptide mixture 9–12 better than to control (no peptides). They produced both IFN-γ (Fig. 2B, *upper panels*) and TNF-α (Fig. 2B, *lower panels*). The expanded CD4 T cells responded very weakly to the peptide mixtures 13–16 and 17–20 by producing TNF-α but not IFN-γ. No responses were observed against the peptide mixtures 1–4 or 5–8 (Fig. 2B). These data indicate that the epitope of HBZ recognized by CD4 T cells from the patient was present in peptides 9–12, within HBZ aa residues 81–130 (Fig. 1).

Next, PBMCs from the same patient were stimulated with four synthetic peptides: 9, 10, 11, and 12. The expanded CD4 T cells responded to peptide 12 by producing both IFN-γ (Fig. 2C, *upper panels*) and TNF-α (Fig. 2C, *lower panels*). The cells did not respond significantly to the other peptides (9, 10, or 11). These results narrow down the specific epitope of HBZ recognized by the CD4 T cells from the patient to a sequence within peptide 12: HBZ aa 111–130 (Fig. 1).

Determination of the minimum epitope sequence of HBZ recognized by CD4 T cells

Seven synthetic peptides (12-1, 12-2, 12-3, 12-4, 12-5, 12-6, 12-7) representing parts of peptide 12 were prepared (Fig. 3A). Responses of the CD4 T cells, which had been stimulated by peptide 12, to these different peptides were tested. The expanded CD4 T cells responded better to peptides 12, 12-1, 12-2, 12-3, and 12-4

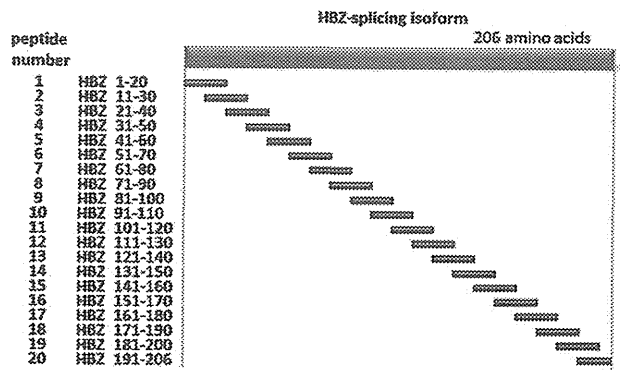

FIGURE 1. Synthetic peptides derived from spliced HBZ. Schematic of 19 20-mer and 1 16-mer synthetic peptides overlapping by 10 aa and covering the entire sequence of the spliced HBZ protein.

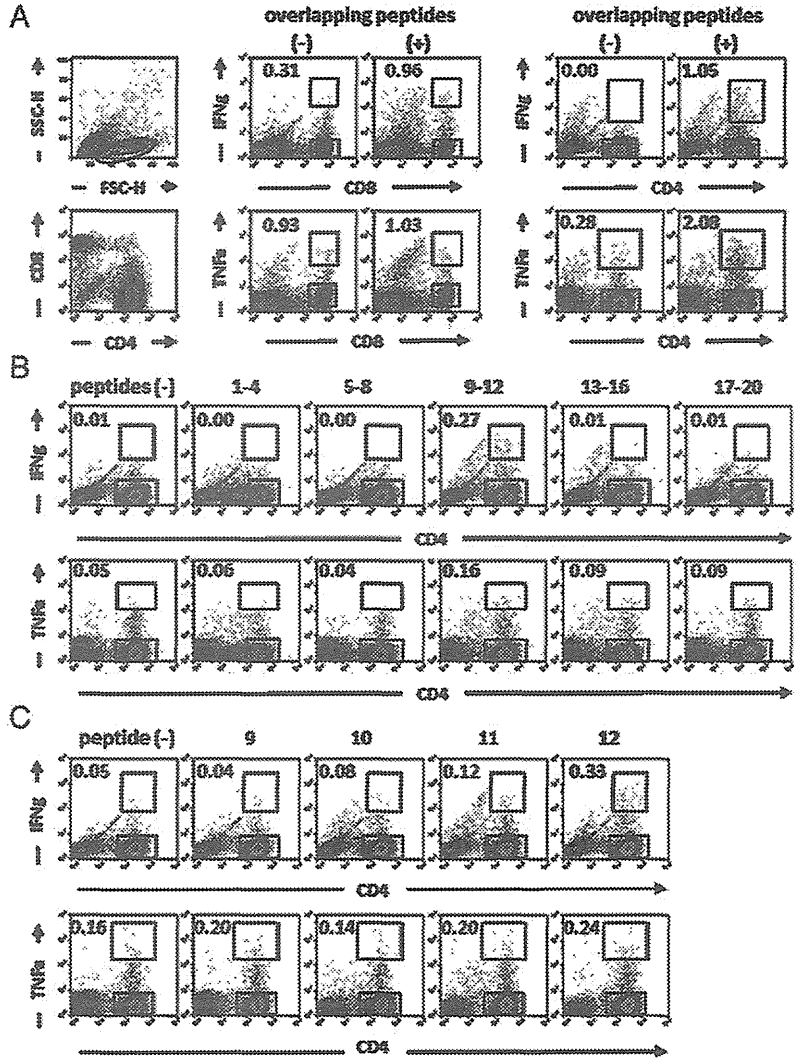

FIGURE 2. T cell responses against synthetic peptides overlapping by 10 aa and covering the entire sequence of the spliced HBZ protein. (**A**) PBMCs from patient #1 after HCT were expanded by stimulating with a mixture of 19 20-mer and 1 16-mer synthetic peptides overlapping by 10 aa and covering the entire sequence of the spliced HBZ protein. The responses of expanded CD8 and CD4 T cells to each of the overlapping peptides were evaluated by the production of IFN-γ or TNF-α. The percentage of responding cells in the upper gate ($CD8^+$ or $CD4^+$ and IFN-γ^+ or TNF-α^+ cells) relative to the cells in the lower gate ($CD8^+$ or $CD4^+$ and IFN-γ^- or TNF-α^- cells) is indicated in each flow cytometry panel. (**B**) PBMCs from patient #1 after HCT were expanded by stimulating with five overlapping peptide mixtures consisting of peptides 1–4, 5–8, 9–12, 13–16, and 17–20. (**C**) PBMCs from patient #1 after HCT were expanded by stimulating with four synthetic peptides: 9, 10, 11, and 12. The responses of expanded CD4 T cells to each synthetic peptide were evaluated by the production of IFN-γ or TNF-α. The percentage of responding cells in the upper gate relative to the cells in the lower gate is indicated in each flow cytometry panel. Each result is representative of three independent experiments.

by producing both IFN-γ and TNF-α. These cells did not respond to peptides 12-5, 12-6, or 12-7 (Fig. 3B). These data indicate that the N terminus of the minimum epitope sequence of HBZ recognized by the CD4 T cells from the patient is arginine, located at HBZ114 (Fig. 3A). Because the expanded CD4 T cells responded to peptide 12-4, the C terminus of the minimum epitope sequence of HBZ must be inside of alanine, located at HBZ125.

Next, three synthetic peptides (12-4-1, 12-4-2, 12-4-3; sequences were HBZ114–124, HBZ114–123, and HBZ114–122, respectively) were prepared to determine the C terminus of the minimum epitope sequence of HBZ (Fig. 3C). The expanded CD4 T cells responded to peptides 12-1 and 12-4 (positive controls) but not to 12-4-1, 12-4-2, 12-4-3, or a negative control peptide 12-7 (Fig. 3D). These data demonstrate that the minimum epitope sequence of HBZ recognized by the CD4 T cells from the patient was RRRAEKKAADVA (HBZ114–125).

Determination of the HLA allele on which the identified HBZ-derived peptides are presented to CD4 T cells

We investigated whether HBZ-specific CD4 T cells also recognized naturally processed and presented peptides. Thus, we initially determined *HBZ* expression by ATL or HTLV-1–immortalized cell lines and found that it was expressed by all of the lines tested (ATN-1, MT-1, MT-2, MT-4, TL-Su, TL-Om1, ATL102), regardless of their *Tax* mRNA expression (Fig. 4A, below the graph). *HBZ* expression levels of these established lines were almost as high as those of PBMCs containing >50% ATL cells obtained from 12 patients with the acute or chronic type of disease. K562 did not express *HBZ*, as might be expected, and all primary ATL cells tested were HBZ^+, consistent with an earlier study (Fig. 4A) (25). Next, we assessed the expression of HLA class II by the cell lines. The ATL or HTLV-1–immortalized cell lines tested were all positive for both HLA-DR and HLA-DQ (Fig. 4B). These observations indicate that ATN-1, MT-1, MT-2, MT-4, TL-Su, TL-Om1, and ATL102 had the potential to present the HBZ-derived peptides on their HLA-DR or HLA-DQ molecules.

Next, we examined the responses of HBZ-specific CD4 T cells from patient #1 after HCT against K562 or HBZ-expressing lines of different HLA types. The responses of HBZ-specific CD4 T cells to the lines were evaluated without the addition of peptide. The CD4 T cells that had been expanded from patient #1 after HCT using peptide 12 responded to peptide 12-1 (positive control) but not to K562, which expressed no *HBZ* (negative control) (Fig. 4C, *upper six panels*). When tested against ATL or HTLV-1–immortalized cell lines, the CD4 T cells responded strongly to ATN-1 and TL-Su (Fig. 4C, *lower panels*). Comparing the HLA class II types of the donor of the effector CD4 T cells (patient #1 after HCT) with ATN-1 and TL-Su showed that HLA-DRB1*15:01 and

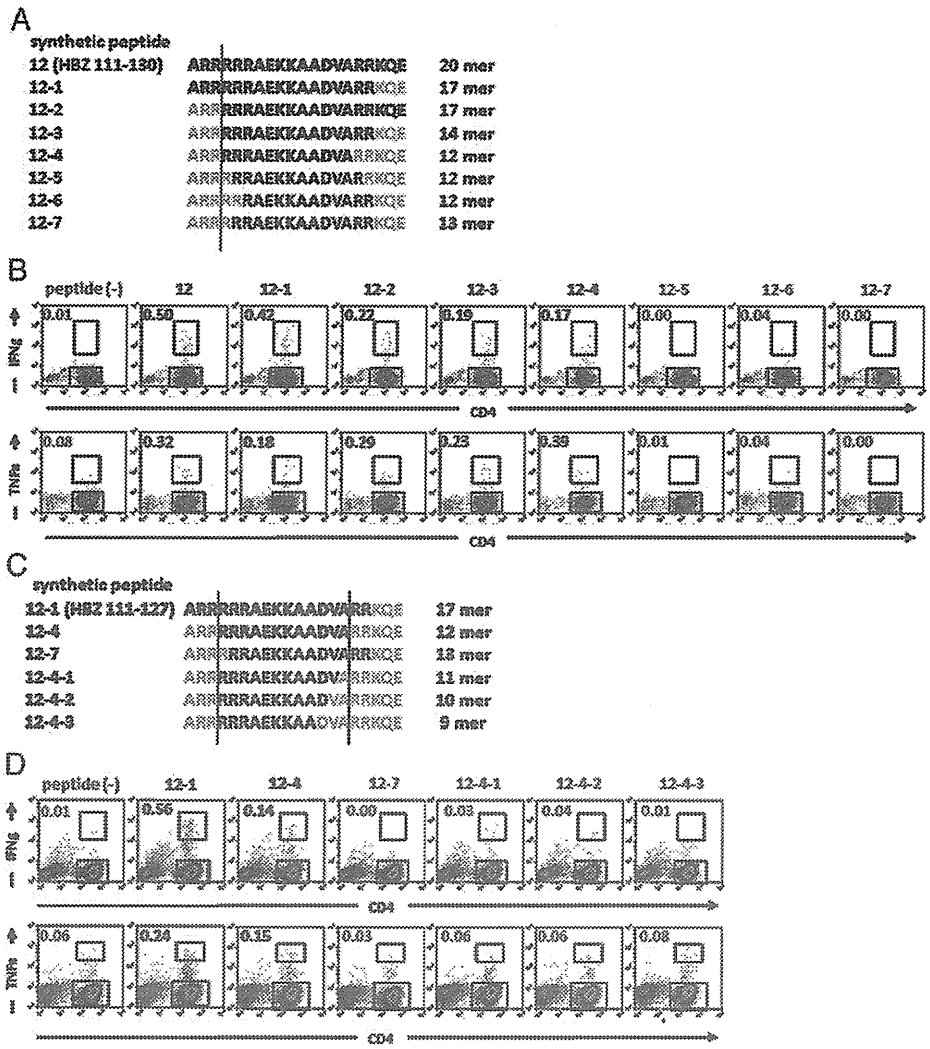

FIGURE 3. Determination of the minimum epitope sequence of HBZ recognized by CD4 T cells. (**A**) Schematic diagram of seven synthetic peptides (12-1, 12-2, 12-3, 12-4, 12-5, 12-6, 12-7) from peptide 12. They were prepared to determine the N terminus of the sequence representing the minimum epitope of HBZ recognized by the CD4 T cells. (**B**) PBMCs from patient #1 after HCT were expanded by peptide 12. The responses of expanded CD4 T cells to each synthetic peptide (12, 12-1, 12-2, 12-3, 12-4, 12-5, 12-6, 12-7) were evaluated by the production of IFN-γ or TNF-α. The percentage of responding cells in the upper gate relative to the cells in the lower gate is indicated in each flow cytometry panel. Each result is representative of three independent experiments. (**C**) Schematic diagram of three synthetic peptides (12-4-1, 12-4-2, 12-4-3) prepared to determine the C terminus of the sequence representing the minimum epitope of HBZ recognized by the CD4 T cells. (**D**) The responses of expanded CD4 T cells to each synthetic peptide (12-1, 12-4, 12-7, 12-4-1, 12-4-2, 12-4-3) were evaluated by the production of IFN-γ or TNF-α. The percentage of responding cells in the upper gate relative to the cells in the lower gate is indicated in each flow cytometry panel. Each result is representative of three independent experiments.

HLA-DQB1*06:02 were shared by all three (Table I). In addition, the CD4 T cells responded to MT-2, TL-Om1, and ATL102 to a lesser degree (Fig. 4C, *lower panels*); these three lines were found to share HLA-DRB1*15:02 and HLA-DQB1*06:01 (Table I). Together, these results indicate that the HBZ-specific CD4 T cell responses from patient #1 after HCT were restricted by HLA-DRB1*15:01 or HLA-DQB1*06:02, as well as by HLA-DRB1*15:02 or HLA-DQB1*06:01. In contrast, the peptide-sensitized CD4 T cells did not respond to MT-1 or MT-4 (Fig. 4C, *lower panels*), consistent with the present observations that the epitope of HBZ recognized by such CD4 T cells was restricted by HLA-DRB1*15:01/HLA-DQB1*06:02 and HLA-DRB1*15:02/HLA-DQB1*06:01.

Next, we tested whether HLA-DR or HLA-DQ restricted the presentation of the HBZ-derived peptide. CD4 T cells expanded by peptide 12 no longer responded to specific stimulation by peptide 12 in the presence of anti–HLA-DR–blocking mAb by producing IFN-γ (Fig. 5A, *upper left panels*), but it did respond in the presence of the isotype-control mAb (Fig. 5A, *upper right panels*). These CD4 T cells also still responded to peptide 12 in the presence of anti–HLA-DQ–blocking mAb (Fig. 5A, *lower left panels*) and its isotype control (Fig. 5A, *lower right panels*). In addition, in the presence of anti–HLA-DR–blocking mAb, CD4 T cells expanded by peptide 12 no longer responded to ATN-1 (Fig. 5B, *left panels*), which carried HLA-DRB1*15:01/HLA-DQB1*06:02 (Table I) and expressed *HBZ* mRNA (Fig. 4A). However, they did respond by producing IFN-γ and TNF-α in the presence of the isotype control (Fig. 5B, *left panels*). These CD4 T cells also still responded to ATN-1 in the presence of anti–HLA-DQ–blocking mAb and its isotype control (Fig. 5B, *right panels*). Furthermore, HBZ-specific CD4 T cell responses to K562 (negative control) were not affected by anti–HLA-DR, anti–HLA-DQ, or their isotype mAbs (Fig. 5C). These observations from Ab-blocking experiments, together with the results shown in Fig. 4, indicate that the epitope sequence of HBZ recognized by the CD4 T cells from patient #1 after HCT were restricted by HLA-DR, specifically HLA-DRB1*15:01 and HLA-DRB1*15:02.

Clinical significance of the specific CD4 T cell response against HBZ

The data presented thus far pertained to CD4 T cells obtained from only one patient (patient #1 after HCT). Therefore, we used HBZ peptide 12 to stimulate and expand 28 PBMC samples obtained from 27 other HTLV-1–infected individuals who carried HLA-DRB1*15:01 or HLA-DRB1*15:02. PBMCs were obtained from 10 HTLV-1 ACs, 10 ATL patients who had not undergone allogeneic HCT, and 8 ATL patients after allogeneic HCT. Among them, PBMCs from one individual (patient #2) were tested at different disease stages (i.e., CRs before and after allogeneic HCT). HBZ-specific CD4 T cell responses were absent in all 10

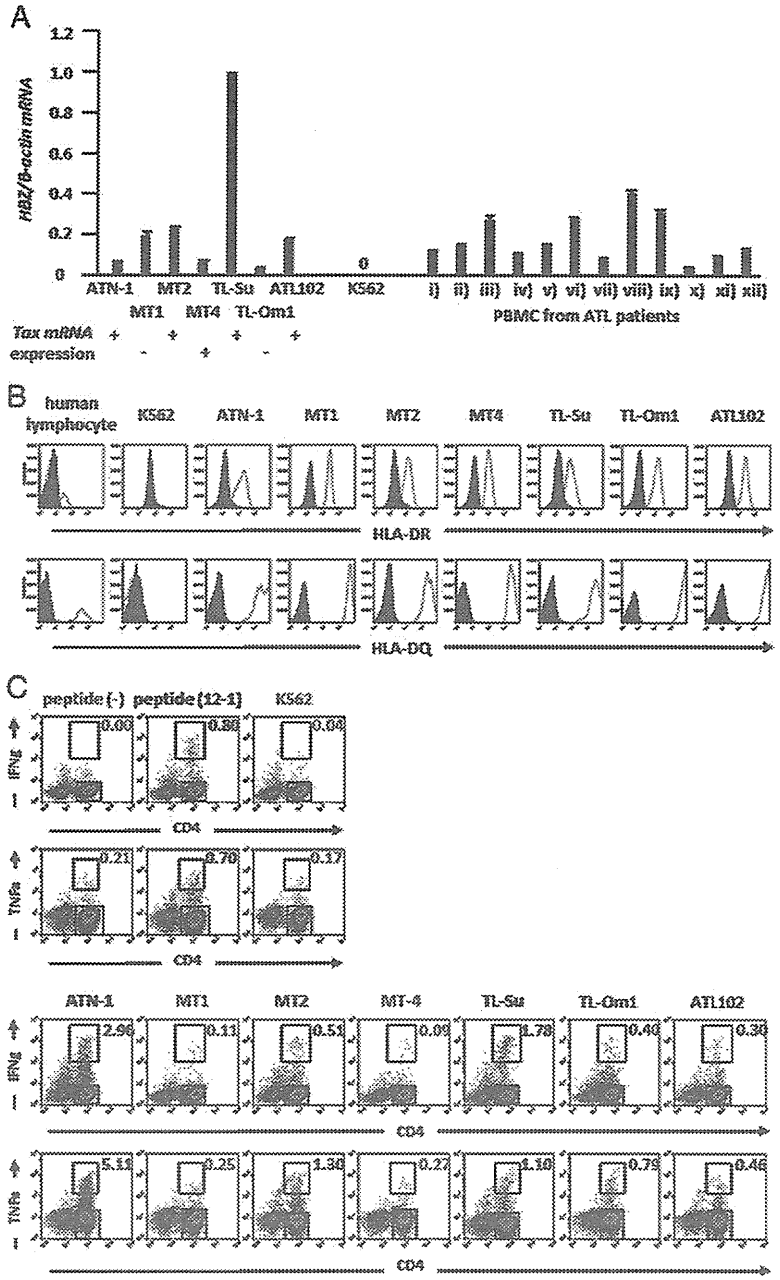

FIGURE 4. Responses of HBZ-specific CD4 T cells from patient #1 after HCT to ATL or HTLV-1–immortalized cell lines. (**A**) *HBZ* expression in ATL and HTLV-1–immortalized cell lines, K562, or PBMCs from ATL patients was analyzed by qRT-PCR by dividing the *HBZ* expression level by the *β-actin* expression level, resulting in an *HBZ/β-actin* mRNA ratio with the expression level in TL-Su set at unity. Data shown are means of triplicate experiments; error bars represent SD. *Tax* mRNA expression of each ATL and HTLV-1–immortalized cell line is indicated, as determined in our previous study (8). (**B**) HLA-DR and HLA-DQ expression in ATL cell lines, HTLV-1–immortalized lines, or K562, as analyzed by flow cytometry. The cell lines were stained with anti–HLA-DR mAb (*upper panels*, open graphs), anti–HLA-DQ mAb (*lower panels*, open graphs), or the corresponding isotype-control mAbs (filled graphs). (**C**) The expanded CD4 T cells were cocultured or not with the synthetic peptide 12-1. Negative controls without peptide stimulation (*upper left panels*) and positive controls with peptide stimulation (*upper middle panels*) are shown. The expanded CD4 T cells were cocultured with target cell lines in the absence of peptide stimulation. CD4 T cells did not respond to K562, which expressed no HBZ and acted as the negative control (*upper right panels*). The CD4 T cell responses to ATL or HTLV-1–immortalized cell lines, which expressed *HBZ*, with different HLA types were evaluated (*lower panels*). The percentage of responding cells in the upper gate relative to the cells in the lower gate is indicated in each flow cytometry panel. Each result is representative of three independent experiments.

HTLV-1 ACs, as well as in all 10 nontransplanted ATL patients (of whom 9 were in CR after systemic chemotherapy and the other was of smoldering type under observation only). In contrast, specific CD4 T cell responses to HBZ were observed in three of the eight additional ATL patients who were in CR after allogeneic HCT (patients #2, #3, and #4). The CD4 T cells from patient #2 and #4 after HCT responded to HBZ peptide 12 by producing both IFN-γ and TNF-α (Fig. 6, *right panels*). In patient #3, no TNF-α response was observed, but there was a clear IFN-γ response to HBZ peptide 12 (Fig. 6, *lower left panels*). Thus, specific CD4 T cell responses against HBZ were observed in four of nine recipients after allogeneic HCT (44%) but in no other ATL patients. Among the patients examined in this study, one patient with acute-type ATL received systemic chemotherapy and achieved CR. Subsequently, she received allogeneic HCT from an HLA-A, B, DR-matched HTLV-1 noninfected sibling donor and maintained CR (patient #2 after HCT). Although HBZ-specific CD4 T cell responses were not present at CR before allogeneic HCT in this patient (Fig. 6, *upper left panels*), they developed after transplantation (Fig. 6, *upper right panels*).

Table I. HLA information

	HLA-DRB1		HLA-DQB1		HLA-DPB1	
ATN-1	*04:05	*15:01	*04:01	*06:02	*05:01	*05:01
MT-1	*04:01	*09:01	*03:01	*03:03	*04:02	*05:01
MT-2	*04:04	*15:02	*03:02	*06:01	*05:01	*09:01
MT-4	*01:01	*16:02	*05:01	*05:02	*05:01	*05:01
TL-Su	*09:01	*15:01	*03:03	*06:02	*02:01	*17:01
TL-Om1	*15:02	*15:02	*06:01	*06:01	*09:01	*09:01
ATL102	*04:04	*15:02	*03:02	*06:01	*05:01	*09:01
Patient #1 after HCT	*04:05	*15:01	*04:01	*06:02	*02:01	*06:01